Received: 29 April 2018 | Revised: 21 February 2019 | Accepted: 16 April 2019

DOI: 10.1111/gcb.14726

PRIMARY RESEARCH ARTICLE

Global Change Biology WILEY

Nitrate addition stimulates microbial decomposition of organic matter in salt marsh sediments

Ashley N. Bulseco[1,2] | Anne E. Giblin[2] | Jane Tucker[2] | Anna E. Murphy[1] | Jonathan Sanderman[3] | Kenly Hiller-Bittrolff[4] | Jennifer L. Bowen[1]

[1]Department of Marine and Environmental Sciences, Marine Science Center, Northeastern University, Nahant, Massachusetts

[2]The Ecosystems Center, Marine Biological Laboratory, Woods Hole, Massachusetts

[3]Woods Hole Research Center, Falmouth, Massachusetts

[4]Department of Biology, University of Massachusetts Boston, Boston, Massachusetts

Correspondence
Jennifer L. Bowen, Department of Marine and Environmental Sciences, Marine Science Center, Northeastern University, MA 01908.
Email: je.bowen@northeastern.edu

Funding information
Division of Environmental Biology, Grant/Award Number: DEB0213767, DEB1350491, DEB1354494 and DEB1701748; Ford Foundation; Division of Ocean Sciences, Grant/Award Number: OCE0423565, OCE0923689, OCE0924287, OCE1058747, OCE1353140 and OCE1637630; Woods Hole Sea Grant, Woods Hole Oceanographic Institution, Grant/Award Number: NA140AR4170074; NSF DDIG, Grant/Award Number: 1701748; NSF FMSL, Grant/Award Number: DBI 1722553

Abstract

Salt marshes sequester carbon at rates more than an order of magnitude greater than their terrestrial counterparts, helping to mitigate climate change. As nitrogen loading to coastal waters continues, primarily in the form of nitrate, it is unclear what effect it will have on carbon storage capacity of these highly productive systems. This uncertainty is largely driven by the dual role nitrate can play in biological processes, where it can serve as a nutrient-stimulating primary production or a thermodynamically favorable electron acceptor fueling heterotrophic metabolism. Here, we used a controlled flow-through reactor experiment to test the role of nitrate as an electron acceptor, and its effect on organic matter decomposition and the associated microbial community in salt marsh sediments. Organic matter decomposition significantly increased in response to nitrate, even at sediment depths typically considered resistant to decomposition. The use of isotope tracers suggests that this pattern was largely driven by stimulated denitrification. Nitrate addition also significantly altered the microbial community and decreased alpha diversity, selecting for taxa belonging to groups known to reduce nitrate and oxidize more complex forms of organic matter. Fourier Transform-Infrared Spectroscopy further supported these results, suggesting that nitrate facilitated decomposition of complex organic matter compounds into more bioavailable forms. Taken together, these results suggest the existence of organic matter pools that only become accessible with nitrate and would otherwise remain stabilized in the sediment. The existence of such pools could have important implications for carbon storage, since greater decomposition rates as N loading increases may result in less overall burial of organic-rich sediment. Given the extent of nitrogen loading along our coastlines, it is imperative that we better understand the resilience of salt marsh systems to nutrient enrichment, especially if we hope to rely on salt marshes, and other blue carbon systems, for long-term carbon storage.

KEYWORDS

16S rRNA gene, anaerobic respiration, decomposition, flow-through reactor, microbes, nitrate, organic matter, salt marsh

1 | INTRODUCTION

Carbon dioxide (CO_2) concentrations continue to rise as a result of fossil fuel burning and land-use changes, thereby contributing to increases in global temperature, ocean acidification, and sea level rise. While a number of carbon capture strategies have been proposed, recent mitigation effort has focused on sequestering CO_2 in blue carbon habitats (Dargusch & Thomas, 2012), which include salt marshes, mangroves, and seagrass meadows (Mcleod et al., 2011; Nelleman et al., 2009). Salt marshes are particularly efficient at storing carbon due to high levels of primary production, the ability to trap organic rich sediments (Chmura et al., 2003), and low rates of microbial decomposition due to largely anaerobic conditions below the first few millimeters of the surface (Reddy & Patrick Jr., 1975). They can bury carbon at rates more than an order of magnitude greater than that of their terrestrial counterparts, over timescales of thousands of years (Duarte, Middelburg, & Caraco, 2005; Mcleod et al., 2011). As such, they have become a major focus of coastal restoration projects (Macreadie et al., 2017; Warren et al., 2002).

Salt marshes face several anthropogenically driven threats that can diminish, and potentially reverse, their capacity to store carbon. Here, we focus on the role of coastal nitrogen (N) inputs, which continue to increase in many systems due to fertilizer production, agricultural and urban runoff, enriched groundwater, and atmospheric deposition (Galloway, Leach, Erisman, & Bleeker, 2017). While salt marshes can remove some of this anthropogenic N before entry into the coastal ocean, either by assimilation into plant biomass (Valiela & Teal, 1974) or conversion to gaseous products (NO, N_2, N_2O) via denitrification or anammox (Hopkinson & Giblin, 2008; Kaplan, Valiela, & Teal, 1979; Koop-Jakobsen & Giblin, 2009), it is unclear how much N loading salt marshes can withstand without having negative implications for carbon storage. Other processes, such as dissimilatory nitrate reduction to ammonium (DNRA), also compete for NO_3^- in anoxic marsh sediments (Brunet & Garcia-Gil, 1996); however, this form of NO_3^- reduction results in retention as NH_4^+ rather than removal as N_2 gas.

In general, salt marshes are considered more resilient to N loading when compared to other coastal systems because of their ability to efficiently remove N (Valiela & Cole, 2002). There is considerable evidence that nutrient enrichment stimulates aboveground primary production (Kaplan et al., 1979; Logan, 2018; Morris, Sundareshwar, Nietch, Kjerfve, & Cahoon, 2002; Vivanco, Irvine, & Martiny, 2015), which facilitates sediment trapping and marsh accretion (Morris et al., 2002) and augments the carbon sink potential by adding biomass. Other studies have also observed increased belowground production in response to elevated N (Pastore, Megonigal, & Langley, 2017). In some systems, however, responses to N enrichment diminished carbon storage capacity. These responses include lost root biomass, increased belowground microbial respiration, and changes in species composition, all of which can result in lower sediment stability and potential marsh collapse (Deegan et al., 2012; Langley, Mozdzer, Shepard, Hagerty, & Megonigal, 2013; Wigand, Brennan, Stolt, Holt, & Ryba, 2009). Due to these complexities, the direction of the response of the marsh carbon storage capacity to increased N loading remains unclear.

One plausible explanation for conflicting observations among marsh fertilization experiments may be the form of N that is applied. Many studies cover small spatial scales and apply N in its reduced form, ammonium (NH_4^+) or urea, although some use a mix of oxidized and reduced forms, ammonium nitrate (NH_4NO_3). In contrast, much of the N delivered to the coastal zone occurs in its oxidized form, nitrate (NO_3^-; Galloway et al., 2008). In addition to supporting primary production through assimilation by marsh vegetation, benthic microalgae, and phytoplankton, NO_3^- can serve as a thermodynamically favorable electron acceptor to fuel microbial oxidation of organic matter (OM) through various anaerobic respiration processes, including denitrification (Hamersley & Howes, 2005; Kaplan et al., 1979) and DNRA (Giblin et al., 2013; Thamdrup & Dalsgaard, 2002). Sulfate (SO_4^{2-}) is another important electron acceptor in salt marsh sediments, accounting for up to 70%–90% of total sediment respiration (Howarth, 1984; Howarth & Teal, 1979) due to its virtually unlimited supply from incoming seawater. However, these two electron acceptors are different thermodynamically in that reducing NO_3^- releases more free energy ($\Delta G°H_2$ = −420 kJ) than reducing SO_4^{2-} ($\Delta G°H_2$ = −98.9 kJ; Canfield, Thamdrup, & Kristensen, 2005). Increased NO_3^- availability, which is typically limiting in coastal systems (Ryther & Dunstan, 1971), may therefore affect the microorganisms using these electron acceptors, and consequently alter the ecosystem functions they mediate.

The mechanisms by which this change in function could occur include: (a) a shift in total microbial community structure to an alternative state better fit for a high NO_3^- environment through changes in electron acceptor availability and competitive exclusion, (b) alteration of metabolic capacity of the existing microbial community to N-cycling metabolisms due to high physiological plasticity, or (c) some combination of the two (Allison & Martiny, 2008; Meyer, Lipson, Martin, Schadt, & Schmidt, 2004; Shade et al., 2012). Regardless of the mechanism, prior studies in salt marsh systems suggest functional responses to NO_3^- do occur through increases in microbial respiration (Deegan et al., 2012), stimulated rates of denitrification (Koop-Jakobsen & Giblin, 2010), and changes to the active bacterial community (Kearns et al., 2016), including through enrichment of nitrous oxide–related genes (Angell et al., 2018; Graves et al., 2016).

These responses are important because NO_3^- reducers, as well as other microbes adapted to high N environments, may oxidize complex forms of OM as a result of greater energy yield from NO_3^- reduction (Beauchamp, Trevors, & Paul, 1989) or from increased production of extracellular enzymes responsible for catalysis and breakdown of complex compounds (Allison, Weintraub, Gartner, & Waldrop, 2010; Treseder, Kivlin, & Hawkes, 2011) when compared to SO_4^{2-} reducers, a group largely limited to simple compounds such as H_2 and acetate (Achtnich, Bak, & Conrad, 1995). As a result, greater NO_3^- availability may affect the biological accessibility of OM by alleviating restrictions to microbial degradation of particular substances. Microbes that reduce NO_3^- may also simply

outcompete other microbes for available electron donors by exploiting the high redox potential (Froelich et al., 1979; Zehnder & Stumm, 1988), resulting in decreased taxonomic diversity and altered function. Considering the fundamental role microbes play in carbon decomposition, and more indirectly, long-term carbon storage (Benner, Newell, Maccubbin, & Hodsin, 1984; Falkowski, Fenchel, & Delong, 2008), it is essential to tease apart which of these mechanisms controls microbial and ecosystem response to NO_3^- addition, as changes in the microbial community may result in the decomposition of OM that would otherwise remain stabilized in the sediment.

To better quantify the role of marshes in long-term carbon storage, it is critical to understand how these systems respond to increasing NO_3^- concentrations. In this study, we investigated whether NO_3^- addition increases the decomposition of salt marsh OM. To explicitly address this question, we implemented a controlled flow-through reactor (FTR) experiment, where we exposed salt marsh sediments to elevated levels of NO_3^-. We hypothesized that the addition of NO_3^- would stimulate the decomposition of OM when compared to unamended sediments, because it is a thermodynamically more favorable electron acceptor. We predicted that this experiment would reveal the presence of a "NO_3^--accessible" pool of OM that microbes could only oxidize under high NO_3^- conditions. We also hypothesized that the depth of OM would play a role in salt marsh sediment response to NO_3^- addition, with lower rates of decomposition in deeper sediment, where OM is less amenable to microbial oxidation due to more complex OM chemical structure. Specifically, we predicted that there would be little difference in decomposition between the NO_3^- and unamended treatments in shallow sediments, since the OM there would be recently deposited and more biologically available for both SO_4^{2-} and NO_3^- reduction, but that there would be a greater stimulation of decomposition at depth in the NO_3^- treatment compared to the unamended sediments. Lastly, we hypothesized that these changes in metabolic function would result from a shift in the microbial community toward taxa better adapted to use NO_3^- in metabolic functions, such as denitrification and DNRA.

2 | MATERIALS AND METHODS

2.1 | Sample collection

We assessed the effect of NO_3^- on the decomposition of sediment OM of varying quality by using samples collected along a depth gradient from salt marsh sediments located in West Creek, part of a marsh complex located in Plum Island Sound, MA (42.759 N, 70.891 W). West Creek is a relatively pristine reference site monitored as part of a long-term nutrient enrichment experiment (Deegan et al., 2007). We collected three replicate cores (5 cm diameter and 30 cm deep) from the tall ecotype of *Spartina alterniflora*, a habitat that floods daily and is under water approximately 35% of the time (Deegan et al., 2007). After we transported the cores back to the laboratory, we stored them at 4°C for 24 hr until the start of the experiment. We sectioned each core into shallow (0–5 cm), mid (10–15 cm), and deep (20–25 cm) sediments and homogenized sections under anoxic conditions. We chose these depths to include OM of varying quality, ranging from relatively newly deposited OM (shallow), to deeper OM found both within (mid) and beyond (deep) the rooting zone. Based on accretion rates taken from nearby sites, we estimate that these sediments range from 50 to 100 years in age (Forbrich, Giblin, & Hopkinson, 2018; Wilson et al., 2014). We removed as much live and dead root material as possible from the homogenized cores using forceps while still working under anoxic conditions, and then split each sectioned depth into a plus-NO_3^- and an unamended treatment (filtered seawater). This resulted in three replicates for each treatment at each depth.

2.2 | FTRs and experimental design

The FTR experimental system (Figure S1) is a modified version of the system described in Pallud, Meile, Laverman, Abell, and Van Cappellen (2007) and Pallud and Van Cappellen (2006). In contrast to whole-core batch incubations or sediment slurries, FTRs provide biogeochemical rate measurements at steady-state conditions and prevent dissolved metabolic by-products from accumulating in the system. Each FTR consists of two Plexiglas® caps that are radially scored for uniform flow, sealed with O-rings to prevent leakage, and has a volume of 31.81 cm^3. We confirmed unilateral, homogenous flow in each reactor using the conservative tracer, bromide, in breakthrough experiments (see supplemental methods for details and Table S1 and Figure S2 for flow property results).

Under anoxic conditions, we loaded each reactor with homogenized sediment, and randomly assigned each reactor a treatment, so that half of the reactors received the plus-NO_3^- treatment (+NO_3^- in 0.2 μm filtered seawater) and half received the unamended treatment (0.2 μm filtered seawater only, representing natural salt marsh conditions). To prepare the two treatment reservoirs, we filtered (0.2 μm) seawater collected from Woods Hole, MA. We sparged the filtered seawater in each of the two reservoirs with N_2 gas until they reached anoxic conditions, which we confirmed using a handheld Hach HQ30D dissolved oxygen meter (Hach Products, Loveland, OH), and spiked the NO_3^- treatment reservoir with 500 μmol/L additional $K^{15}NO_3^-$ (Cambridge Isotope Laboratories, Andover, MA). We acknowledge that 500 μmol/L is high when compared to natural conditions, ranging from approximately two to five times higher than porewater concentrations found in other nutrient-enriched marshes (e.g., Negrin, Spetter, Asteasuain, Perillo, & Marcovecchi, 2011; Peng et al., 2016). However, our goal was to compare sediment OM decomposition under NO_3^- enriched and unamended conditions rather than to compare to field rates. Therefore, it was critical that NO_3^- be available to microbes through the entire thickness of the reactors in our enriched treatment. We initially added 350 μmol/L for the first 25 days, but found that all the NO_3^- was being fully consumed. At this point, we increased the concentration to 500 μmol/L.

The reactors received treatment seawater at a targeted flow rate of approximately 0.08 ml/min (see Table S1 for measured flow rate) using peristaltic pumps rigged with 0.89 mm (inner diameter) MasterFlex FDA viton tubing (Cole Parmer, IL). We then carried out a 92 day experiment in a glove bag flushed with N_2 gas and confirmed anoxic conditions by continuously bubbling each reservoir with N_2 and monitoring oxygen concentrations using a handheld Hach HQ30D dissolved oxygen meter. Once the reactors reached steady state at the 10 day mark, we collected samples from both reservoirs and effluent throughout the remainder of the experiment to measure changes in biogeochemical parameters and to monitor flow rate. To assess changes in OM composition and microbial community structure, we homogenized and aliquoted bulk sediment from the start of the experiment (pretreatment) and from sediment in each reactor at the end of the experiment. We dried bulk sediments overnight at 65°C before freezing at −20°C, and immediately flash froze additional aliquots of sediments in liquid nitrogen for nucleic acid extraction and stored them at −80°C until further analysis.

2.3 | Biogeochemical and OM analyses

We collected water samples approximately every 10 days from both the plus-NO_3^- and unamended reservoirs along with all reactor outflows to measure biogeochemical processes resulting from microbial activity. Samples for DIC, sulfide, and gases were collected in glass tubes placed in-line in the outflow with no headspace and water for nutrients was collected in acid-washed 15 ml conical tubes. To assess total microbial respiration, we measured dissolved inorganic carbon (DIC; CO_2 + HCO_3 + CO_3^{2-}) on an Apollo SciTech AS-C3 DIC analyzer (Newark, DE) following methods in Dickson and Goyet (1994). We measured nitrate + nitrite (NO_3^- + NO_2^-) via chemiluminescence on a Teledyne T200 NOx analyzer (Teledyne API, San Diego, CA) following methods outlined in Cox (1980), and measured ammonium (NH_4^+) and sulfide colorimetrically on a Shimadzu 1601 spectrophotometer (Kyoto, Japan) following protocols from Solórzano (1969) and Gilboa-Garber (1971), respectively. To calculate the production and consumption rates of each analyte (DIC, NO_3^-, NH_4^+, and sulfide) over time, we calculated the difference in concentration between the inflow (reservoir) and the outflow (effluent), corrected for flow rate in L/hr, and divided by reactor volume (31.81 cm^{-3}) for each sampling point. Because we were not able to measure changes in SO_4^{2-} due to high seawater concentrations and proportionally minor changes resulting from experimental conditions, we determined that sulfate reduction was occurring through the production of sulfide (HS^-) and calculated a conservative total sulfate reduction rate (SRR) by taking the sum of HS^- produced and total S storage measured at the end of the experiment (described below). We also calculated the DIC:NH_4^+ ratio to draw general inferences about OM pools being decomposed based on C:N stoichiometry.

We determined the relative contribution of competing NO_3^- reduction pathways to total NO_3^- consumption in the plus-NO_3^- treatment only by measuring the production of labeled N_2 from $^{15}NO_3^-$ tracer as dissolved gas on a membrane inlet mass spectrometer (MIMS; Kana et al., 1994) connected to a copper column heated to 600°C to remove oxygen interferences (Eyre, Ryshaard, Dalsgaard, & Christensen, 2002; Lunstrum & Aoki 2016). To determine anammox and denitrification, we monitored the production of $^{29}N_2$ and $^{30}N_2$, respectively, and calculated rates using the following equation (Nielsen, 1992),

$$D_{15} = p29 + 2p30 \quad (1)$$

where D_{15} is denitrification from $^{15}NO_3^-$, and $p29$ and $p30$ correspond to the production of $^{29}N_2$ and $^{30}N_2$. To measure DNRA, we bubbled water samples with helium for 10 min to remove any N_2 gas and converted $^{15}NH_4^+$ produced from DNRA to $^{29}N_2$ and $^{30}N_2$ using a hypobromite iodine solution following the OX/MIMS method (Yin, Hou, Liu, Liu, & Gardner, 2014). We measured gases on the MIMS and calculated DNRA rates as:

$$\mathrm{DNRA}_{15} = p29 + 2p30. \quad (2)$$

It was not necessary to calculate denitrification from $^{14}NO_3^-$ using the isotope pairing method (Nielsen, 1992) because we only added NO_3^- in the form of $^{15}NO_3^-$, and ambient NO_3^- concentrations were largely below detection. We also considered the production of $^{14}NO_3^-$ from nitrification to be negligible, as this is primarily an aerobic process (Herbert, 1999), and we maintained constant anoxia throughout this experiment.

To assess geochemical changes in OM, we dried samples at 65°C and fumed samples with 12N HCl before performing elemental composition analysis (percent carbon and nitrogen) on a Perkin Elmer 2400 Series Elemental Analyzer (Perkin Elmer, Billerica, MA) using acetanilide as a standard. We dried additional samples at 105°C overnight to obtain water content and used these data to calculate bulk density of each reactor assuming a volume of 31.81 cm^3. Lastly, we obtained percent sulfur (%S) by combusting dried samples at 1,350°C and measuring sulfur dioxide (SO_2) production on a LECO S635 S analyzer (LECO Corporation, Saint Joseph, MI).

To further characterize changes in OM as a result of NO_3^- addition, we used Fourier Transform-Infrared Spectroscopy (FT-IR), a technique that provides rapid, detailed information about the relative abundance of chemical functional groups. To prepare samples for FT-IR analysis, we finely ground sediment dried at 40°C for 48 hr. We ran each sample on a Bruker Vertex 70 Fourier Transform-Infrared Spectrometer (Bruker Optics Inc., Billerica, MA) outfitted with a Pike AutoDiff diffuse reflectance Accessory (Pike Technologies, Madison, WI) and obtained data as pseudo-absorbance (log[1/reflectance]) in diffuse reflectance mode. We collected at a 2 cm^{-1} resolution with 60 coadded scans per spectrum at the mid-IR range, from 4,000 to 400 cm^{-1}, using a mirror for background correction. Resulting raw spectra were transformed using a calculated two-point linear tangential baseline using Unscrambler X (Camo Software, version 10.1, Woodbridge, NJ) and then assigned peaks according to Margenot, Calderón, Boweles, Parikh, and Jackson (2015) and Parikh, Goyne, Margenot, Mukome, and Calderón (2014) as outlined in Table S2.

2.4 | Nucleic acid extraction, amplification, and amplicon sequencing

We extracted genomic DNA from approximately 0.25 g wet sediment using the MoBio® PowerSoil DNA Isolation Kit (MoBio Technologies, CA) following manufacturer's instructions, and eluted the DNA into a 35 µl final volume. We amplified in triplicate the V4 region of the 16S rRNA gene using the general bacterial primer-pair 515F (5′-GTGCCAGCMGCCGCGGTAA-3′) and 806R (5′-GGACTACHVGGGTWTCTAAT-3′; Caporaso et al., 2011) with Illumina adaptors (Caporaso et al., 2012) and individual 12-bp GoLay barcodes on the reverse primer, using the following reaction: 10 µl 5-Prime Hot Master Mix (Quanta Bio, Beverly, MA), 0.25 µl of 20 µM forward and reverse primers, 13.5 µl DEPC-treated water, and 1 µl of DNA template. PCR cycling conditions follow those outlined by the Earth Microbiome Project (Caporaso et al., 2011). Prior to sequencing, we gel purified the pooled PCR product using a Qiagen® QIAquick gel purification kit (Qiagen, Valencia, CA) and quantified the resulting purified product using a Qubit® 3.0 fluorometer (Life Technologies, Thermo Fisher Scientific, Waltham, MA). After pooling to equimolar concentrations, we performed sequencing on the Illumina MiSeq (Illumina, San Diego, CA) platform using a 300-cycle kit and V2 chemistry. All reads are deposited in the NCBI Sequence Read Archive under accession number PRJNA505917.

2.5 | Statistical analyses

We conducted all statistical analyses in R unless otherwise stated (R Core Team, 2019) and used an alpha of 0.05 for all significance testing. To investigate changes in DIC production over time, we performed a linear regression on each core using weeks since start of the experiment as the explanatory variable and DIC production rate as the dependent variable. We integrated between sampling points to calculate the cumulative flux of DIC, NH_4^+ production, sulfur storage, and total SO_4^{2-} reduction across the duration of the experiment and tested for significant differences in DIC, NH_4^+ production, sulfur storage, and total SO_4^{2-} reduction, as a function of treatment and depth, using a two-way ANOVA. For both NO_3^- consumption and sulfide production, detectable only in the plus-NO_3^- or unamended treatments, respectively, we assessed differences among depths using a one-way ANOVA. We also compared denitrification and DNRA among depths using a one-way ANOVA, and compared these rates to each other using a two-sample *t* test. We assessed the contribution of these two dissimilatory processes to NO_3^- consumption by calculating a ratio of denitrification and DNRA over total NO_3^- reduction. Similarly, we performed a mass balance between DIC and SRR in both the plus-NO_3^- and unamended treatments. To account for differences in bulk carbon supply on DIC production, we calculated total carbon loss by taking the proportion of carbon released as DIC divided by the total mass of carbon per reactor using sediment characteristic data (e.g., water content and %C).

To assess changes in %C, %N, bulk density, and %S throughout the experiment, we calculated the difference between initial and final sediments per core and compared these changes among treatment and depth using a two-way ANOVA. We performed a principal coordinate analysis (PCoA) across entire FT-IR spectra and used a PERMANOVA with 999 permutations to test for significant differences by treatment and depth using Manhattan distance to construct the resemblance matrix from the FT-IR data. To further visualize trends in these data, we also plotted the Pearson's correlation coefficients against wavenumber to determine which spectral bands best explained the distribution of sample scores in the PCoA based on functional group assignments in Table S2. Lastly, we calculated the ratio of aromatic carbon (1,650 cm^{-1}) to carboxyl functional groups (1,270 cm^{-1}), where higher values imply a greater extent of decomposition (Keiluweit, Wanzek, Kleber, Nico, & Fendorf, 2017), and used a two-way ANOVA to compare these ratios as a function of treatment and depth.

To investigate bacterial community composition, we analyzed sequence data in QIIME 2 (version 2017.12). We demultiplexed a total of 1,521,493 16S rRNA gene sequences across all samples and inferred amplicon sequence variants (ASVs) using the DADA2 plugin (Callahan et al., 2016) with a maxEE of 2 and the consensus chimera removal method. Quality filtering resulted in an average of 37,381 (±6,693) sequences per sample. We then assigned taxonomy with the Greengenes 16S rRNA sequence database (version 13-8; McDonald et al., 2012) and removed ASVs occurring only once (singletons) and any sequences matching chloroplasts and mitochondria. After aligning sequences using MAFFT v7 (Katoh & Standley, 2013), we performed beta diversity analysis with weighted UniFrac (Lozupone, Iladser, Knights, Stombaugh, & Knight, 2011) on ASV tables normalized to 22,999 sequences (which was our lowest sequencing depth), and tested for significant differences among treatments and depth using PERMANOVA with 999 permutations. To examine within sample diversity, we calculated a Shannon diversity index with these normalized data and tested for differences across treatment and depth using a two-way ANOVA. We ran a random forest model from the randomForest R package (v4.6-12; Liaw & Wiener, 2002) using 10,000 trees on a filtered feature table containing ASVs present at least 100 times (186 ASVs total) to identify taxa most important in classifying between plus-NO_3^- and unamended treatments. To confirm model results, we examined the out-of-bag error rate (a method that uses bootstrap aggregation to assess performance without a training set) and performed leave-one-out cross-validation with 999 permutations in the caret R package (v6.0-73; Kuhn, 2016). We then plotted the relative abundance of ASVs most important in correctly classifying between treatments as a heatmap, and clustered samples using unweighted pair group method with arithmetic mean (UPGMA) on Euclidean distances (Michener & Sokal, 1957).

3 | RESULTS

3.1 | Biogeochemical rates

Across all depths, the addition of NO_3^- resulted in higher DIC production rates (microbial respiration; Figure 1) and total cumulative

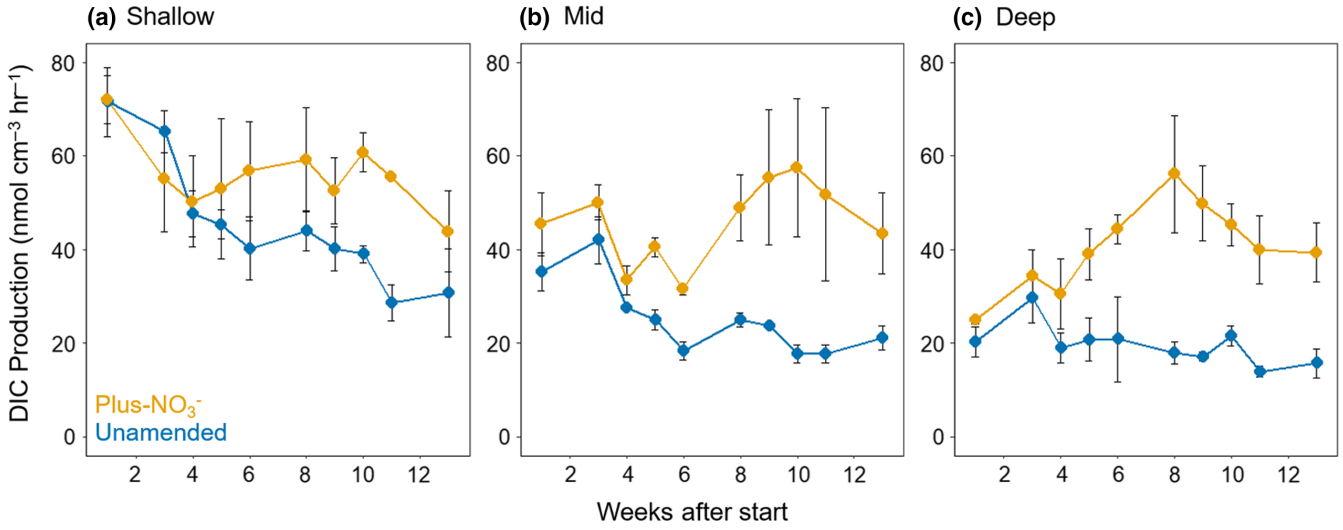

FIGURE 1 Average (±*SE*) dissolved inorganic carbon (DIC) production over time (weeks) across three depths that correspond to different ages of marsh organic matter (panels a–c; n = 3)

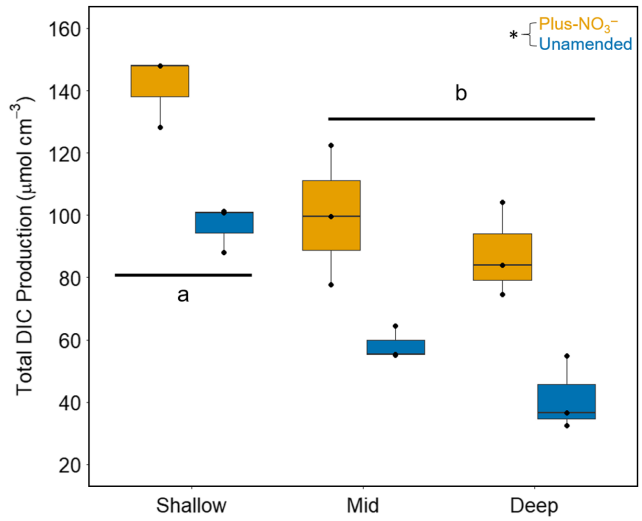

FIGURE 2 Average (±*SE*) cumulative dissolved inorganic carbon (DIC) production over 92 days in µmol/cm^3 for nitrate and unamended treatments at each depth. Boxes represent 25%–75% quartiles, where the solid black line is the median value and the whiskers are upper and lower extremes. Black dots represent values for each individual reactor. A two-way ANOVA indicates a significant effect of treatment (p < 0.001, $F_{1,14}$ = 21.73) and depth (p < 0.001, $F_{2,14}$ = 48.33) on total DIC production, but there was no significant interaction between the two. Letters represent statistically different DIC production by depth from a Tukey's HSD test corrected for multiple comparisons test and the asterisk indicates a significant difference between treatments at all depths

production (Figure 2) compared to the unamended treatment, both over time and at the end of the experiment. In both treatments, total DIC production decreased with depth (Figure 2), with shallow sediments exhibiting significantly greater microbial respiration than mid and deep sediments. While DIC production rates decreased over the duration of the experiment in the shallow, unamended sediments (Figure 1a; linear regression; p = 0.002, $F_{1,18}$ = 12.87, R^2 = 0.38), no such pattern existed in the plus-NO_3^- treatment.

In the plus-NO_3^- treatment, the sum of DNF and DNRA accounted for 102.5 ± 0.15%, 91.3 ± 4.4%, and 95.1 ± 14.0% of total NO_3^- consumption (Figure 3). Background NO_3^- concentrations in the incoming seawater were consistently low (0.6–1.2 µM), and although all of this NO_3^- was removed throughout the experiment in the unamended treatment, the low initial concentrations resulted in negligible NRR. In the plus-NO_3^- treatment, NRR ranged from 14.6 to 87.2 µmol cm^{-3} hr^{-1} (Figure 3), with cumulative rates of 97.4 ± 1.4 µmol/cm^3, 77.2 ± 5.6 µmol/cm^3, and 72.5 ± 13.1 µmol/cm^3 for shallow, mid, and deep sediments, respectively. Cumulative NO_3^- reduction did not significantly differ by depth (p = 0.16); however, elevated rates in the shallow sediments corresponded to greater rates of DIC production (Figure 2). Cumulative denitrification rates were 70.6 ± 1.0 µmol/cm^3, 58.1 ± 2.2 µmol/cm^3, and 55.2 ± 5.9 µmol/cm^3 for shallow, mid, and deep sediments, respectively; however, differences by depth were not significant (p = 0.054). DNRA rates were significantly higher in the shallow sediments (29.2 ± 1.3 µmol/cm^3) compared to the mid (11.8 ± 0.7 µmol/cm^3) and deep (10.7 ± 3.1 µmol/cm^3) sediments (p < 0.001, $F_{2,6}$ = 27.29), but overall, DNRA rates were not as high as denitrification rates at any depth (p < 0.001, t = 17.17).

Sulfide production, used together with total S in sediment as a measure of SRR, occurred at all depths in the unamended treatment and was significantly higher in shallow compared to deep sediments (Figure 4a,b). Sulfide concentrations, in contrast, were undetectable in the plus-NO_3^- treatment. Changes in S storage indicated that SO_4^- reduction was occurring in both treatments (Figure 4c), although SRR was lower in the plus-NO_3^- treatment than in the unamended sediments. There was a significant interaction between treatment and depth on SRR, with the unamended treatment exhibiting more SO_4^{2-} reduction than the plus-NO_3^- treatment in shallow sediments, and unamended shallow sediments exhibiting more SO_4^{2-} reduction than the unamended mid

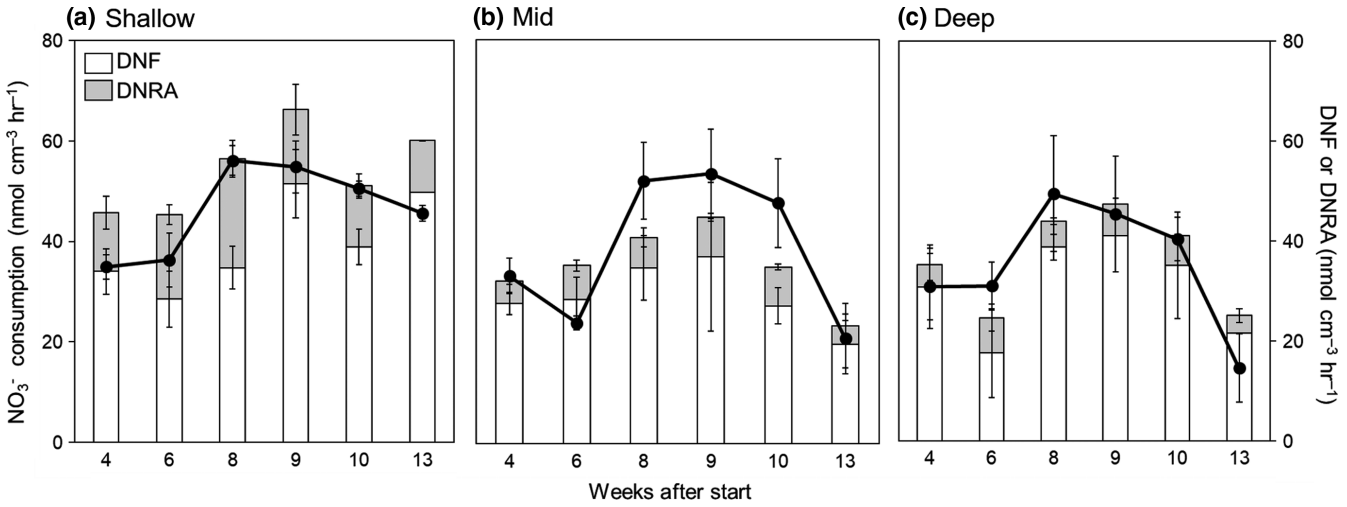

FIGURE 3 NO_3^- consumption in proportion to denitrification and dissimilatory nitrate reduction to ammonium (DNRA). Black line represents average (±*SE*) nitrate consumption rates over time (weeks) and stacked bar plots indicate average (±*SE*) rates of denitrification (DNF; white) and dissimilatory nitrate reduction to ammonium (DNRA; gray). A one-way ANOVA indicated DNRA was signficantly higher in shallow sediments compared to mid and deep sediments ($p < 0.001$, $F_{2,6} = 27.29$), while there was no significant pattern in denitrification by depth ($p = 0.054$). Rates of denitrification were greater than DNRA across all depths according to a two-sample *t* test ($p < 0.001$, $t = 17.17$)

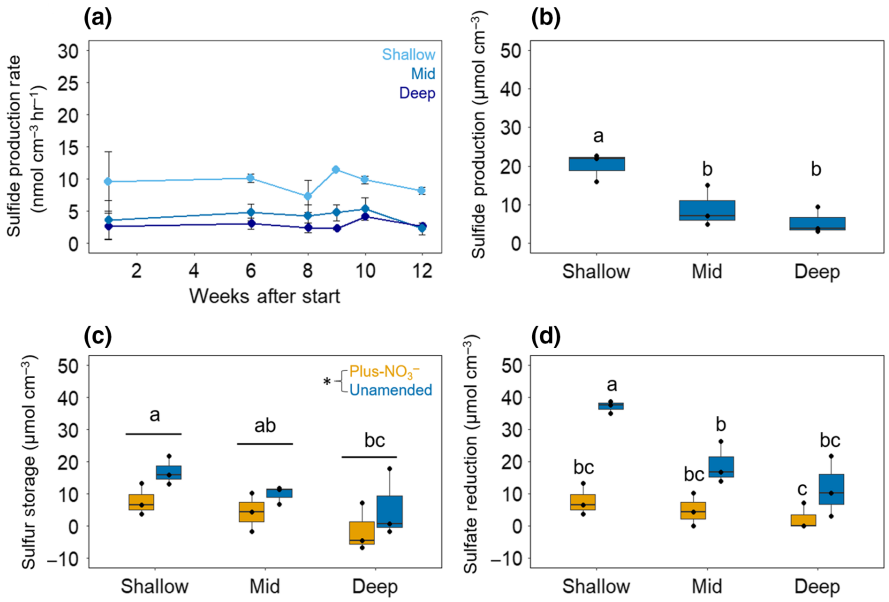

FIGURE 4 (a) Average (±*SE*) sulfide production rates over time (weeks) and (b) total sulfide production. One-way ANOVA indicated shallow sediments exhibited significantly greater sulfide production than mid and deep sediments ($p = 0.012$, $F_{2,6} = 9.96$). Changes in sulfide were undetectable in the plus-NO_3^- treatment and were thus not included in panels a and b. (c) A two-way ANOVA indicated that total sulfur storage was greater in the unamended treatment across all depths (as indicated by an asterisk; $p = 0.024$, $F_{1,14} = 7.64$), with deep sediments exhibiting less storage than shallow sediments ($p = 0.037$, $F_{2,14} = 4.21$). (d) There was a significant interaction between treatment and depth on total sulfate reduction (sulfide + sulfur production; $p = 0.029$, $F_{2,12} = 4.81$). Letters represent statistically different sulfate reduction from a Tukey's HSD test corrected for multiple comparisons

and deep sediments (Figure 4d). Overall, based on stoichiometry, SO_4^- reduction accounted for 76.8 ± 1.4%, 64.2 ± 9.3%, and 59 ± 30.8% of total DIC production in the unamended treatment, and 15.0 ± 3.8%, 9.4 ± 8.4%, and 1.6 ± 8.5% in the plus-NO_3^- treatment for shallow, mid, and deep sediments, respectively.

There was no significant difference in NH_4^+ production between treatments; however, shallow sediments produced significantly more NH_4^+ when compared to mid and deep sediments in both the plus-NO_3^- and unamended treatments (Figure 5). In addition, the DIC:NH_4^+ ratio was significantly higher in the plus-NO_3^- treatment, while in the unamended treatment, the ratio remained consistently low across all depths (Figure 6) and was similar to the C:N value of sediments from the start of the experiment (13.66 ± 0.69).

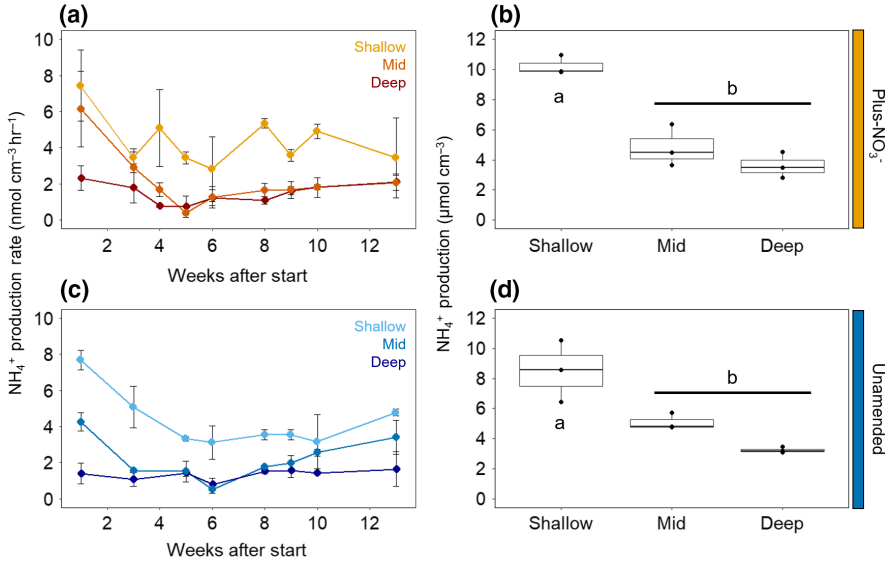

FIGURE 5 Average (±*SE*) ammonium production rates over time (days) in the nitrate (a) and unamended (c) treatments, and total ammonium production in µmol/cm^3 across depth for nitrate (b) and unamended (d) treatments. While there was no effect of treatment, a one-way ANOVA indicated a significant effect of depth (nitrate (b): $p < 0.001$, $F_{2,6} = 37.47$; unamended (d): $p = 0.005$, $F_{2,6} = 14.09$), as indicated by a Tukey's HSD test corrected for multiple comparisons

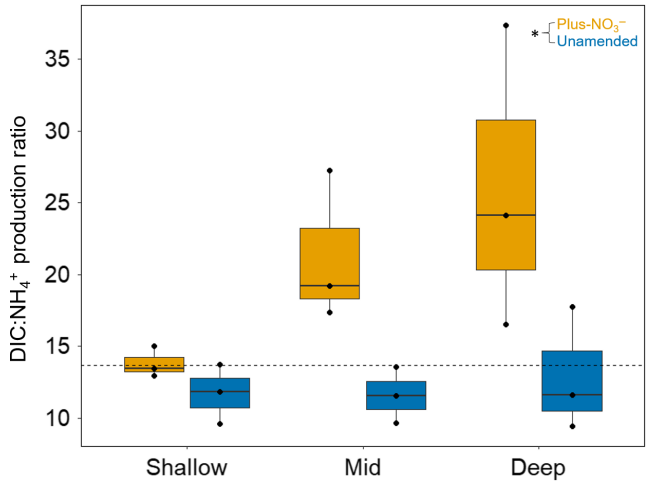

FIGURE 6 The ratio of dissolved inorganic carbon (DIC) to ammonium production calculated per core was greater in the plus-NO_3^- treatment compared to unamended sediments as indicated by the asterisk ($p = 0.007$, $F_{1,14} = 10.11$), while depth was insignificant ($p = 0.147$), according to a two-way ANOVA. The dotted line indicates the average C:N ratio of sediments from the start of this experiment (13.66 ± 0.69)

3.2 | Organic matter

Molar C:N of preexperiment sediments demonstrated an increasing trend with depth, ranging from 13.1 ± 0.5, 13.6 ± 0.3, and 14.2 ± 0.6 for shallow, mid, and deep sediments, respectively (Figure 7a), but this trend was not statistically significant ($p = 0.195$). We compared change in %C, %N, molar C:N, and S in the plus-NO_3^- and unamended sediments versus sediments collected prior to the experiment (Table 1). There was no significant difference in pre- versus postexperiment carbon or molar C:N between treatments; however, there was a change in %N by depth and total S by depth and treatment, with significantly greater S concentrations in the unamended sediments (Figure 4c).

The proportion of carbon lost as DIC throughout the experiment ranged only from 0.76% to 3.47% of the total carbon in each reactor, so it is not surprising that we did not detect significant changes in most bulk sediment properties between treatments. To observe changes in OM, we applied FT-IR spectroscopy and explored relative shifts in chemical functional groups related to decomposition processes. A principal coordinates analysis (PCoA; Figure 7b) of whole FT-IR spectra using Manhattan distances indicated separation by depth along the first coordinate axis (explaining 77.6% of the variance) and treatment along the second coordinate axis (explaining 22.2% of the variance), both of which were significant according to PERMANOVA analysis (Figure 7b). Pairwise comparisons of mean Manhattan distances further indicated that each depth was significantly different from the rest (shallow–mid, $p = 0.006$, $t = 3.029$; mid–deep, $p = 0.009$, $t = 2.72$; shallow–deep, $p = 0.001$, $t = 5.94$), but when examining treatment, only pretreatment and unamended sediments were significantly different from each other ($p = 0.019$, $t = 2.20$). We next plotted the Pearson's correlation coefficient against wavenumber for the first two factors, which accounted for 99.8% of total variance in the PCoA. This allowed us to identify three functional groups that exhibited the most influence on observed separation along the primary and secondary axes (Figure 7d): Groups that were important in differentiating between treatments included lignin-like compounds at 840 and 1,650 cm^{-1} (Artz et al., 2008), aliphatic carbon at 1,470 cm^{-2}, and polysaccharides at 1,080 cm^{-1}.

To further explore whether a change in carbon chemical structure occurred during the incubation, we calculated the ratio of aromatic carbon (1,650 cm^{-1}) to carboxyl functional groups (1,270 cm^{-1}), where higher values imply a greater extent of decomposition (Keiluweit et al., 2017). A two-way ANOVA of the aromatic:carboxyl group ratio indicated a significant effect of treatment ($p = 0.027$, $F_{2,22} = 4.24$), but not depth ($p = 0.651$), with a higher ratio in the unamended treatment when compared to initial sediments (Figure 7c).

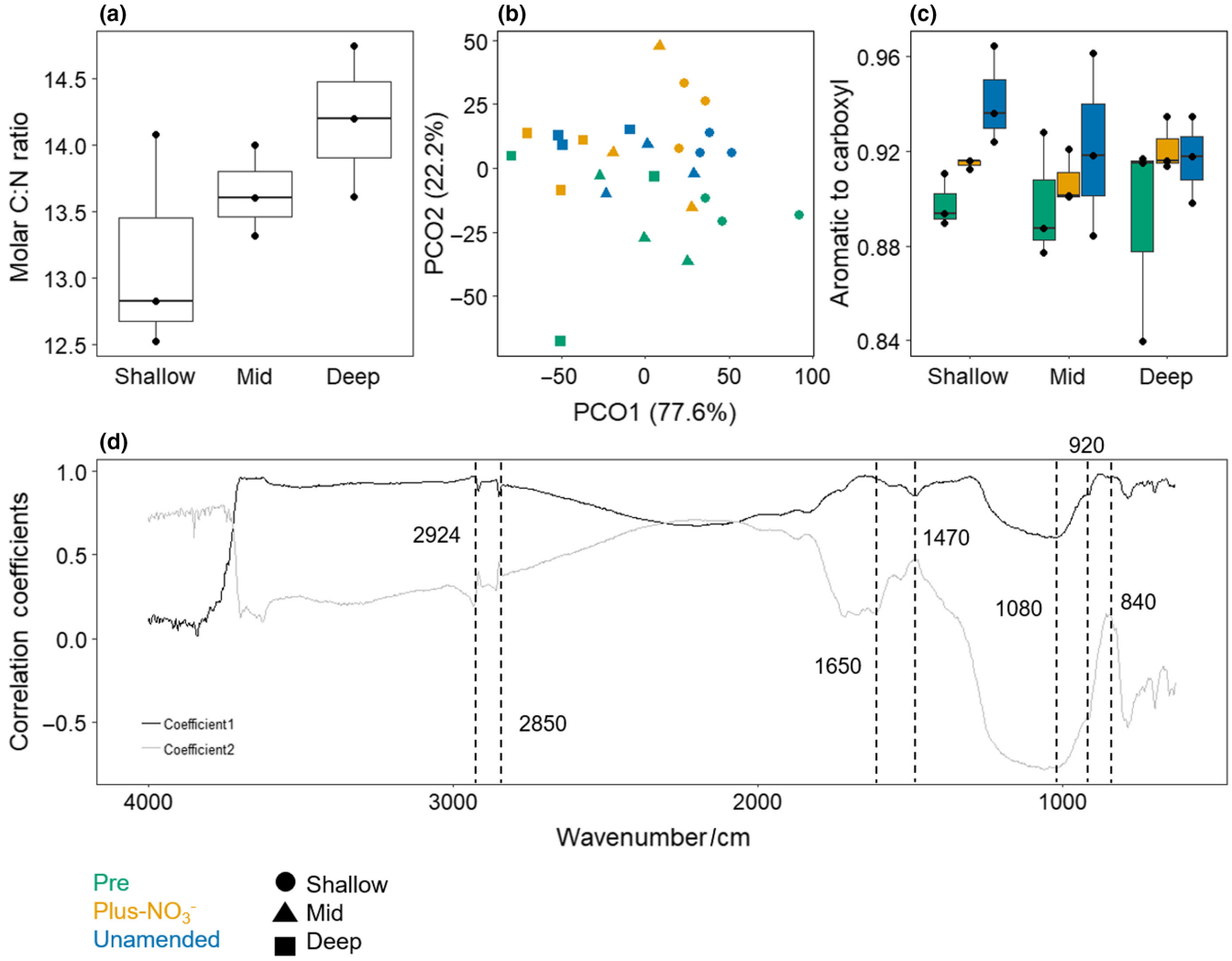

FIGURE 7 (a) Boxplot of molar C:N ratio at each depth before the start of the experiment (b) Principal coordinates analysis (PCoA) of Fourier Transform-Infrared Spectra (FT-IR) indicates significant differences by treatment (PERMANOVA; $p = 0.017$, $F_{2,18} = 3.31$) and depth ($p = 0.001$ $F_{2,18} = 16.60$). (c) A two-way ANOVA of the aromatic:carboxyl group ratio indicated a significant effect of treatment ($p = 0.027$, $F_{2,22} = 4.24$) but not depth ($p = 0.651$), with a higher ratio in the unamended treatment when compared to initial sediments. (d) Pearson's correlation coefficients plotted against wavenumber representing regions most discriminating across two axes shown in (b). Dotted lines indicate functional group assignments listed in Table S2, with 840–920 and 1,650 cm^{-1} = aromatic carbon and lignin-type signatures, 1,080 cm^{-1} = polysaccharides, and 1,470 and 2,850–2,924 cm^{-1} = aliphatic carbon

TABLE 1 Average (±*SE*) bulk density, change in carbon (mg), nitrogen (mg), and sulfur (mg), and final molar C:N per reactor treatment-depth combination ($N = 3$), with negative numbers indicating loss throughout the experiment

	Bulk density	Δ Carbon (mg)	Δ Nitrogen (mg)	Molar C:N	Δ Sulfur (mg)
Unamended					
Shallow	0.22 (0.01)	−141.42 (51.71)	−13.76 (1.2)^{a}	13.24 (0.10)	63.70 (9.99)^{a}
Mid	0.21 (0.01)	−34.69 (13.56)	−6.38 (1.66)^{b}	13.97 (0.27)	39.22 (6.98)^{ab}
Deep	0.22 (0.02)	−41.29 (36.94)	−3.35 (1.24)^{b}	14.17 (0.18)	19.24 (21.15)^{ab}
Nitrate					
Shallow	0.24 (0.02)	−154.12 (60.93)	−13.32 (1.65)^{a}	13.10 (0.09)	25.28 (9.63)^{ab}
Mid	0.22 (0.02)	−91.49 (60.93)	−8.39 (3.90)^{b}	13.71 (0.09)	14.98 (11.38)^{ab}
Deep	0.24 (0.01)	−76.12 (27.05)	−5.55 (2.04)^{b}	14.10 (0.20)	−4.89 (14.31)^{b}

Two-way ANOVA indicates a significant difference in nitrogen lost among depths ($p = 0.002$, $F_{2,14} = 10.42$) but not between treatments, and a significant increase in total S in the unamended treatment ($p = 0.018$, $F_{1,12} = 7.37$) compared to the plus-NO_3^- treatment. Letters represent results from Tukey's HSD test corrected for multiple comparisons.

3.3 | Microbial community composition in response to nitrate

A principal coordinates analysis constructed from Weighted UniFrac similarities revealed a significant effect of both treatment and depth on microbial community composition (Figure 8a). There was a clear separation in community similarity along the primary axis (43.20% of the variance explained) due to NO_3^- addition, and a separation driven primarily by differences between shallow and mid–deep sediments (Figure 8a) along the secondary axis (20.82% of the variance explained). To determine the effect of NO_3^- addition on alpha diversity, we calculated the Shannon Index and found a significant effect of both treatment and depth, but not the interaction of the two factors. Across all depths, alpha diversity was significantly lower in the plus-NO_3^- treatment when compared to the unamended treatment (Figure 8b).

A random forest model, using 10,000 trees and 186 predictor variables derived from the most abundant ASVs, correctly classified microbial communities as belonging to either the plus-NO_3^- or unamended treatment 100% of the time with a 0% out-of-bag error rate. Leave-one-out cross-validation confirmed model performance, with a Cohen's kappa statistic, which compares observed accuracy to expected accuracy due to random chance, of 100%. The top 30 ASVs most important in discriminating between treatments accounted for 45.2% of total sequences and included taxa from Phyla Bacteroidetes, Proteobacteria, Chlorobi, Caldithrix, Chloroflexi, Planctomycetes, Acidobacteria, Gemmatimonadetes, Verrucomicrobia, and candidate group WWE1 (Table S3; Figure 9). Of these 30 ASVs, classes from Flavobacteria, Gammaproteobacteria, Alphaproteobacteria, and Ignavibacteria were more abundant in the plus-NO_3^- treatment, while the unamended treatment was much more diverse, including classes from Deltaproteobacteria, Bacteroidia, Caldithrix, Anaerolineae, Cloacamonae, BPC102, Gemm-2, Phycisphaerae, Epsilonproteobacteria, Alphaproteobacteria, Verrucomicrobiae, and Betaproteobacteria. We also tested the random forest model without excluding rare taxa (but still removing singletons) to see if these rarer ASVs would have a disproportionate influence on the dataset. This also resulted in 100% classification rate and 0% out-of-bag error, but only accounted for an additional 1.9% of all sequences (ASVs 31–41 listed in Table S3).

4 | DISCUSSION

4.1 | DIC production rates decreased with depth

Our study used a controlled FTR experiment to test the effect of OM chemical complexity and NO_3^- addition on microbial respiration. We found that DIC production decreased as a function of depth, with shallow sediments exhibiting significantly greater microbial respiration rates than mid and deep sediments (Figure 2). This pattern was particularly evident in the unamended treatment, where DIC production also decreased throughout the duration of the experiment in the shallow sediments (Figure 1a) likely because accessible OM began to limit SRR (Westrich & Berner, 1984). Decreasing DIC production with depth likely resulted from changes in OM accessibility that also occurs with depth. Microbes preferentially degrade the least complex, highest energy-yielding plant and microalgae-derived OM in surface sediments. Organic components with greater activation energies that are therefore more resistant to degradation in salt marsh environments tend to accumulate over time, and ultimately become buried under newly deposited OM and sediment. These components persist in such environments where their degradation has become thermodynamically unfavorable, as dictated by the sum of processes that impede microbial access to a particular substrate. While microbes can still degrade these OM compounds over time, the process occurs at a much slower rate due to greater

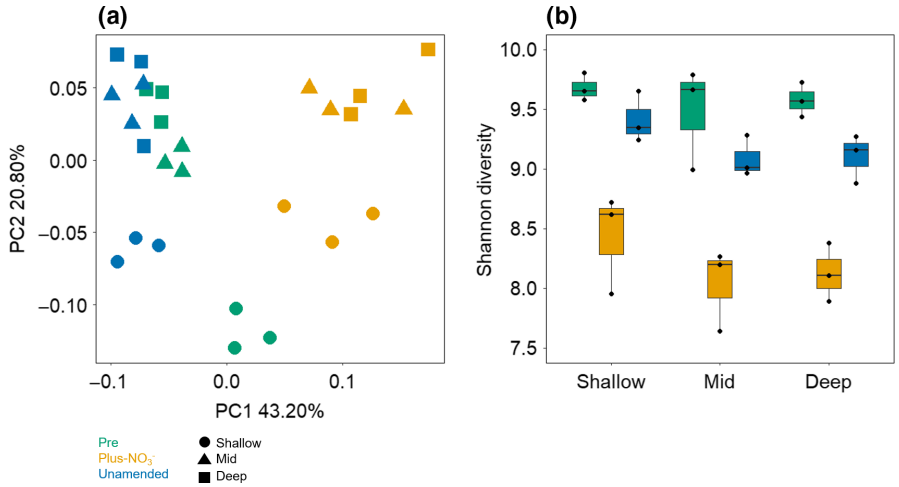

FIGURE 8 (a) Principal coordinates analysis constructed based on weighted UniFrac where color represents sample treatment and shape indicates sample depth. Results from a PERMANOVA indicate significant differences in community composition by treatment (p = 0.001, $F_{2,22}$ = 11.11) and by depth (p = 0.006, $F_{2,22}$ = 3.03). (b) Shannon diversity index. A two-way ANOVA revealed a significant effect of both treatment (p < 0.001, $F_{2,22}$ = 71.21) and depth (p = 0.044, $F_{2,22}$ = 3.61), as indicated by a Tukey's HSD test corrected for multiple comparisons, but no effect of the interaction between the two

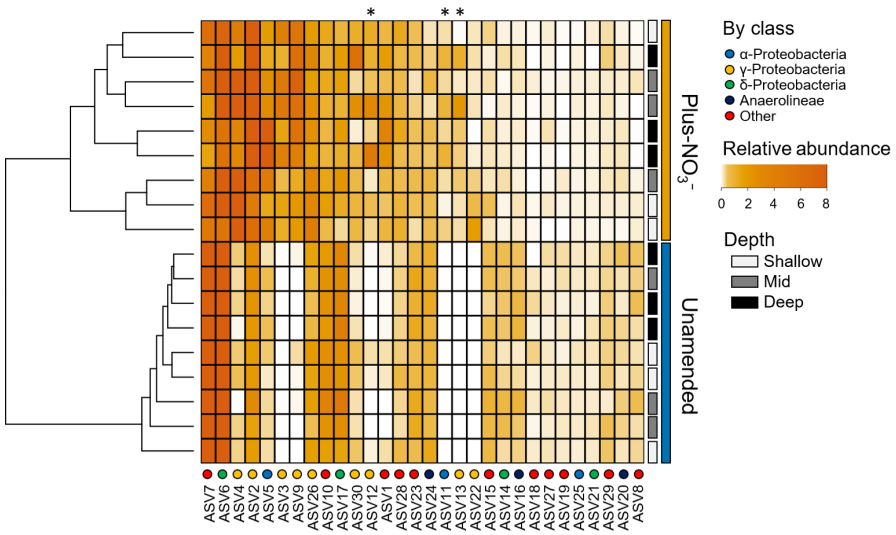

FIGURE 9 Heatmap showing relative abundance of top 30 amplicon sequence variants (ASVs; 45.2% of sequences) most important in correctly discriminating between plus-NO_3^- (top nine rows) and unamended treatments (bottom nine rows) according to a random forest classification model, clustered using an unweighted pair group method with arithmetic mean (UPGMA) on Euclidean distances. Lighter colors indicate less abundant taxa, while darker colors indicate more abundant taxa. Colored circles represent the taxonomic class of each ASV and gray-scale bars indicate sample depth. ASVs marked with an asterisk belong to groups known to carry out dissimilatory nitrate reduction. Additional taxonomic information can be found in Table S3

energetic requirements (Westrich & Berner, 1984) and physical protection from particle aggregation (Brodowski, John, Flessa, & Amelung, 2006; Schmidt et al., 2011). The end result is decreased decomposition rates. Initial bulk sediment %C, molar C:N (Table 1; Figure 7a), and the aromatic:carboxyl group ratio did not differ significantly among the different depths in this experiment. However, FT-IR spectra indicated a significant difference in functional groups (Figure 7b) at different depths driven primarily by polysaccharide depletion (Figure 7d), which suggests increasing OM stability in deeper sediments. The lack of significant differences in bulk sediment ratios emphasizes the importance of using higher resolution techniques to evaluate OM characteristics. By assessing entire FT-IR spectra, we were able to identify relative depletion and accumulation of specific functional groups that resulted from our experimental treatment.

The decrease in DIC production with depth is also, in part, due to decreasing availability of thermodynamically favorable electron acceptors in anoxic marsh sediments. Energetically favorable electron acceptors, such as NO_3^-, are preferentially reduced at the surface and are therefore depleted in deeper sediments (Canfield et al., 2005). While SO_4^{2-} is rarely limiting in most marsh systems due to its high concentration in seawater and delivery via incoming tides (Howarth & Teal, 1979; Jørgensen, 1977), SO_4^{2-} reduction is a much less energetically favorable metabolic pathway, releasing less free energy per mole of carbon oxidized compared to NO_3^- reduction thereby limiting the range of organic compounds that can be degraded. Furthermore, SO_4^{2-} reduction only accounted for 59.0%–76.8% of DIC production, suggesting that other alternative electron acceptors, such as iron and manganese oxides, could have also contributed to microbial respiration (Canfield et al., 2005). However, we did not measure iron or manganese oxides, so cannot comment on patterns regarding these processes.

Since SO_4^{2-} reduction yields less energy and therefore limits the range of organic compounds that can be degraded, rates of decomposition generally decrease with depth where OM has accumulated with time (Arndt et al., 2013; Canfield et al., 2005), though the presence of roots and bioturbation can alter this pattern (Aller & Aller, 1998; Canfield & Farquhar, 2009; Kostka et al., 2002). Decreased decomposition at depth is consistent with the decrease in DIC production (Figure 2) and sulfide production (Figure 4b) we observed in the deeper unamended sediments. In addition, DIC production decreased as a function of time in the shallow unamended treatment (Figure 1), suggesting that after first oxidizing the more biologically available OM compounds, only less accessible OM remained, leading to decreased decomposition rates. This result corroborates other studies that find a strong relationship between OM degradability and SRR, with increasing OM stability resulting in lower decomposition rates regardless of SO_4^{2-} availability (Canfield, 1989; Westrich & Berner, 1984).

4.2 | Evidence for a nitrate accessible pool of OM

The addition of NO_3^- resulted in significantly greater DIC production across all depths, most notably in deeper sediments, where OM is less biologically available for microbial oxidation. While NO_3^- is a thermodynamically favorable terminal electron acceptor that fuels high rates of denitrification and DNRA in salt marshes, it is typically coupled with nitrification at oxic interfaces or rooting zones (Hamersley & Howes, 2005; Howes, Howarth, Teal, & Valiela, 1981), and hence limited at depth where NO_3^- cannot be internally regenerated. By experimentally adding NO_3^- in this experiment, similar to what might occur in coastal environments under high N loading, we

thereby increased NO_3^- availability. In doing so, we increased rates of denitrification (Figure 3) and OM oxidation (Figures 1 and 2), and consequently increased rates of decomposition. These results suggest the existence of a "NO_3^--accessible" OM pool and emphasize that "recalcitrance" of OM as commonly used in the salt marsh literature depends on the environmental context, including both OM accessibility and electron acceptor availability. OM that is considered environmentally recalcitrant under SO_4^{2-}-only conditions may no longer be stable under NO_3^- availability once energetics barriers are overcome.

High NO_3^- conditions may stimulate the microbial community to break down these otherwise stable OM compounds by providing more energy for metabolic processes. Higher DIC:NH_4^+ ratios in the plus-NO_3^- treatment provide support for this claim. In general, more DIC relative to NH_4^+ production indicates that microbes are using OM with higher C:N ratios (Canfield et al., 2005). In the plus-NO_3^- treatment, particularly at depth, the DIC:NH_4^+ ratio was much higher, suggesting that microbial communities may be accessing a different OM pool compared to unamended sediments, in which C:N remained consistently low and very similar to the average sediment ratio from the start of the experiment (Figure 6). It is noteworthy that the ratio of DIC:NH_4^+ in the plus-NO_3^- and unamended treatments was similar in shallow sediments, where OM appears to be accessible to both NO_3^- and SO_4^{2-} reducers. As this ratio diverges between treatments with depth, it provides further evidence for the existence of this separate "NO_3^--accessible" OM pool that microbes can access once NO_3^- limitation is released. There are other processes by which this increasing pattern in DIC:NH_4^+ can emerge, including differences in microbial biomass and N uptake or anammox (Dalsgaard, Thamdrup, & Canfield, 2005; Schmid et al., 2007). Our NH_4^+ data suggest, however, that there were no significant differences in net NH_4^+ production between treatments, given that cumulative NH_4^+ production across the entire experiment was the same (Figure 5). We cannot, however, comment on the potential for gross NH_4^+ production and consumption in our experiment, as our sampling strategy and resolution did not allow for it. We did monitor production of $^{29}N_2$, which showed that anammox was negligible in this experiment, agreeing with other studies conducted in salt marsh sediments (Koop-Jakobsen & Giblin, 2009). We therefore conclude that this increase in DIC:NH_4^+ ratio is most likely explained by the oxidation of a higher C:N pool of OM at depth in the plus-NO_3^- treatment.

FT-IR spectral data also suggest that microbes in the plus-NO_3^- treatment were accessing a different pool of OM than microbes in the unamended treatment. A PCoA of whole FT-IR spectra from 4,000 to 400 cm^{-1} indicated a significant difference in the OM chemistry among depths and between the unamended and pretreatment sediments, but the plus-NO_3^- treatment was not different between the other two (Figure 7a). This result suggests that decomposition not only caused a shift in the OM signature when compared to pretreatment sediments but also the plus-NO_3^- and unamended OM composition shifted in different ways.

Higher aromatic:carboxyl group ratios in the unamended treatment compared to the pretreatment sediments show that microbial OM oxidation resulted in a more stable residual OM pool (Figure 7c); a result that we could not detect in the bulk sediment properties (Table 1). Remarkably, these data also suggest that after incubation, the OM from the unamended treatments was in a state of greater decomposition than the OM from the plus-NO_3^- treatment (Figure 7c), even though the amount of C mineralized was less. This result supports the pattern observed in the PCoA of OM composition, where Manhattan distances indicated a significant difference between pretreatment and unamended sediments, but not the plus-NO_3^- treatment (Figure 7b). One possible explanation for this counterintuitive finding is that NO_3^- addition might facilitate decomposition of more complex OM (e.g., large cyclic compounds such as cellulose), either through fermentation or hydrolysis, which would result in more bioreactive, low-molecular-weight substrates (Beauchamp et al., 1989). Rather than a predictable sequence following thermodynamic theory, which asserts that electron acceptors with higher redox potential are exclusively reduced first (Froelich et al., 1979; Zehnder & Stumm, 1988), these results suggest that NO_3^- supports cometabolism by providing more accessible OM compounds for competing microbial functional groups (Achtnich et al., 1995). This is supported by the existence of some measurable SO_4^{2-} reduction in the plus-NO_3^- treatment, in stark contrast to the inhibition of SRR that would be predicted by thermodynamics (Zehnder & Stumm, 1988). However, since the majority of NO_3^- reduction in the plus-NO_3^- treatment could be accounted for by the sum of denitrification and DNRA (Figure 3), we can conclude that less thermodynamically favorable electron acceptors, such as SO_4^{2-}, iron, and manganese oxides, were not important contributors.

In addition, the fact that the pretreatment and plus-NO_3^- treatment were not significantly different from each other suggests that there is less selective utilization of OM in response to NO_3^-. In the unamended treatment, SO_4^{2-} reducers may have only had access to a limited supply of low-molecular-weight substrates (Canfield et al., 2005), therefore creating a more complex OM pool over time (Figures 1 and 4) and a significant shift in overall chemical composition (Figure 7a). Our data suggest that, with the addition of NO_3^-, microbes were accessing a wider range of compounds; thus, despite greater decomposition rates (Figure 2), there was less of a shift in the overall chemical composition of the remaining OM (Figure 7b). Similar results have been observed in both terrestrial and oceanic studies, with N addition resulting in the selection for microbes that responded to the N supply and that could decompose complex carbon compounds more efficiently (Allison et al., 2013; Campbell, Polson, Hanson, Mack, & Schuur, 2010; Treseder et al., 2011). Another possible explanation for a more bioreactive signature in the plus-NO_3^- treatment is a greater supply of extracellular DNA from greater microbial biomass (e.g., Dell'Anno & Danavaro, 2005); however, since NH_4^+ production rates were similar between treatments at the end of the experiment (Figure 5), this is likely not the case.

Rather than acting as an electron acceptor, another consequence of NO_3^- addition could be the release of the microbial community from nutrient limitation, which may also result in increased DIC production rates due to assimilation and higher growth rates. However,

the majority of NO_3^- reduction in the plus-NO_3^- treatment could be accounted for by the sum of denitrification and DNRA (Figure 3). In addition, most anaerobic microbes are not nutrient limited because their growth-per-unit substrate-intake is much lower than with aerobic respiration (Canfield et al., 2005), which is why typical anoxic porewater nutrient concentrations are higher than those found in oxic sediments. Overall, our data show most of the NO_3^- consumed can be attributed to dissimilatory processes, further supporting the finding that NO_3^- is stimulating decomposition by acting as a thermodynamically favorable electron acceptor.

4.3 | NO_3^- addition effects on microbial community structure

We hypothesized that the end result of NO_3^- addition would be (a) to fundamentally alter the resident microbial community through a change in resources (either electron acceptors or donors) or (b) to alter the function of the existing community through metabolic plasticity of the microbes present (Allison & Martiny, 2008), with both scenarios resulting in shifts in the dominant metabolic pathways. Through 16S rRNA gene sequencing in conjunction with biogeochemical measurements, we found evidence for a combination of the two. While we observed a core microbiome that existed in both the plus-NO_3^- and unamended treatment (Figure S3), including microbial taxa typically present in these particular salt marsh sediments (e.g., Kearns et al., 2016), we also found a significant shift in microbial community structure (Figure 8a) and decreases in alpha diversity (Figure 8b) in response to NO_3^-. This suggests that NO_3^- addition selects for a subset of taxa that are more competitive in a high N environment, representing a community fundamentally different from both pretreatment and unamended sediments, and that these taxa are largely driving increases in decomposition via denitrification.

Through random forest classification analysis, we identified 30 ASVs most important in correctly classifying between plus-NO_3^- and unamended treatments (Figure 9; Table S3). Of these 30 ASVs, ~70% were from the class Gammaproteobacteria, a widely diverse group of gram-negative bacteria that consistently increases in abundance as a result of fertilization (e.g., Campbell et al., 2010; Coolon, Jones, Todd, Blair, & Herman, 2013; Leff et al., 2015). Many of these ASVs were putatively assigned to orders known to reduce NO_3^- (Kiloniellales, Oceanospirillales; Garrity, Bell, & Lilburn, 2005; Wiese, Thiel, Gärtner, Schmaljohann, & Imhoff, 2009), oxidize sulfur/sulfide (Thiotrichales, Chromatiales; Garrity et al., 2005; Imhoff, 2005; Thomas, Giblin, Cardon, & Sievert, 2014), ferment OM (Ignavibacteriales, Rhodospirillales; Biebl & Pfening, 1981; Iino et al., 2010), and degrade high-molecular-weight (HMW) compounds (Flavobacteriales, Thiotrichales, Alteromonadales). Some members of these groups can also use long-chain alkanes (Fernández-Gómez et al., 2013; Guibert et al., 2016) and are stimulated in the presence of HMW-dissolved OM (Mahmoudi et al., 2015; McCarren et al., 2010). These shifts in the community provide evidence for the selection of taxa more adept at using nitrate or oxidizing more complex OM. In contrast, ASVs more abundant in the unamended treatment included orders that are ubiquitous in soil and mangrove sediments (Verrucomicrobiae, Caldithrixales; Freitas et al., 2012; Miroshnichenko, Kolganova, Spring, Chernyh, & Bonch-Osmolovskaya, 2010), that can reduce sulfate (Desulfobacterales, Desulfarculales; Bahr et al., 2005), and that exhibit properties associated with iron metabolism (Campylobacterales, Rhizobiales; Eppinger, Baar, Raddatz, Huson, & Schuster, 2004; Reese, Witmer, Moller, Morse, & Mills, 2013). While we cannot make definitive statements regarding the exact function associated with these taxa, identifying the taxa most responsive to NO_3^- addition is a step forward in understanding the mechanistic response of microbial communities to nutrient enrichment.

4.4 | Assumptions and limitations of FTR experiments

We chose a high concentration of NO_3^- (500 μM NO_3^-) to assure non-limiting concentrations at a reasonable flow rate (Pallud et al., 2007). We designed this experiment specifically to assess the potential of NO_3^- to mobilize carbon pools that were not being oxidized by SO_4^{2-} reduction, rather than to simulate realistic environmental conditions. In the environment, NO_3^- will almost always be limiting except in the most eutrophic conditions or in situations of continuous replacement; therefore, we cannot extrapolate the rates of decomposition observed in this experiment to field conditions. However, we can conclude from our data that adding NO_3^- may stimulate the decomposition of deeper, more chemically complex sediment OM. There exist scenarios where NO_3^- reduction may dominate forms of anaerobic respiration, such as freshwater wetlands or wastewater treatment plants, but it is much less likely to occur naturally in salt marshes where NO_3^- is limiting and there is unlimited supply of sulfate from the tides. Our study suggests that, by adding NO_3^-, NO_3^- reduction does not necessarily become the dominant process, but instead allows for the decomposition of OM that was not being mobilized under conditions of SO_4^{2-} alone.

Furthermore, the use of FTRs eliminates some of the complexity involved with plant–microbe feedbacks and competition for NO_3^- by benthic microalgae and phytoplankton. While these interactions are clearly important in situ, the aim of this experiment was to explicitly examine the role of NO_3^-, in stimulating microbial processes. By splitting core replicates between treatments, we ensured that initial sediment conditions were identical between NO_3^- and unamended sediments; thus, while residual influence of plants may be present in the sediments we collected, these signals should be similar between treatments and therefore not directly influence the patterns we observed. We also assumed that, in our experiment, SO_4^{2-} was the only electron acceptor being supplied in our unamended treatment aside from the very small background concentration of NO_3^- (0.6–1.2 μM) in the seawater we used. We do not believe that this affected the treatment differences. Since background SO_4^{2-} concentrations are so high in seawater (~28 mM), we were not able to detect small changes at the μM level that occurred in the FTRs and

had to instead make conservative estimates of SRR from rates of sulfide production and changes in sediment S concentrations. These changes are likely due to pyrite or FeS formation, although we cannot rule out the production of organic sulfur (Luther III, Church, Scudlark, & Cosman, 1986). Although we did not monitor the influent oxygen concentrations, we conducted the entire experiment in an anoxic glove chamber, so oxygen was not present for either oxic respiration or nitrification. Finally, since this experiment only lasted ~90 days, we cannot determine how large the NO_3^--accessible OM pool is, whether NO_3^- reducers are solely responsible for the stimulation, or if they also stimulate SO_4^{2-} reducers through cometabolism.

4.5 | Implications of N-loading on salt marsh carbon storage capacity

Our results show that NO_3^- addition stimulates DIC production and consequently, the decomposition of OM in salt marsh sediments. We observed this response even in deep sediments, where we traditionally assume OM to be fairly resistant to microbial degradation. We found that by adding NO_3^- and providing a more energetically favorable electron acceptor to the system, the microbial community shifted toward taxa better suited for a high NO_3^- environment with significant impacts on carbon cycling. OM that was stable and unavailable to SO_4^{2-} reducers became at least partially bioavailable under high NO_3^- conditions. These results suggest that comparable additions of NO_3^- to salt marshes could also enhance OM decomposition in situ.

These results could have important implications for salt marsh carbon storage potential. The effect of adding NO_3^- that we demonstrate here would depend on the specific hydrology of the marsh system. If NO_3^--rich flooding waters penetrate into deep sediments via burrows constructed by benthic macroinvertebrates or by entering directly through the sides of the creekbanks into deeper sediments, it could accelerate the decomposition of stored carbon. Not only could this decrease carbon storage potential, it could also result in decreased belowground marsh stability (e.g., Deegan et al., 2012) and lead to greater CO_2 production. Additionally, marsh systems currently experiencing high NO_3^- conditions may store less OM over time, leading to less overall carbon storage; although the OM that is buried may be more resistant to further decomposition, since a larger portion will already be oxidized. What this means for carbon storage potential of marshes at a larger scale is unclear, since NO_3^- can also stimulate OM production by acting as a nutrient, with such production offsetting respiration. Total marsh carbon storage capacity depends heavily on the balance between these two processes. Lastly, by stimulating N-cycling processes, the potential for nitrous oxide (N_2O) production, a greenhouse gas with 263 times the sustained global warming potential of CO_2 (Neubauer & Megonigal, 2015), may also increase as a result of incomplete denitrification (we did not measure N_2O fluxes in this study). Considering the degree of eutrophication in US estuaries (Bricker et al., 2008), and how NO_3^- addition alters processes that control OM, it is important to incorporate our understanding of these processes when assessing the resilience of salt marsh systems to changing climate and increasing anthropogenic pressures. This is especially critical if we hope to rely on salt marshes for long-term carbon storage.

ACKNOWLEDGEMENTS

We thank Joseph Vallino at Marine Biological Laboratory for his invaluable contribution to the design of our flow-through reactor system. We also thank researchers of the TIDE project (NSF OCE0924287, OCE0923689, DEB0213767, DEB1354494, and OCE 1353140) for the maintenance of the long-term nutrient enrichment experiment, as well as researchers of the Plum Island Ecosystems LTER (NSF OCE 0423565, 1058747, 1637630). We acknowledge Sam Kelsey, Khang Tran, Michael Greenwood, and members of the Bowen lab for their assistance in the field and laboratory, as well as Inke Forbrich, Nat Weston, and Gary Banta for their thoughtful comments on this research. This work was funded by a NSF CAREER Award to JLB (DEB1350491), a Woods Hole Oceanographic Sea Grant award to AEG, JJV, and GTB (Project No. NA140AR4170074 Project R/M-65s), and a NSF DDIG Award to JLB and ABM (Award No. 1701748). Resources published with funds from the NSF FMSL program (DBI 1722553 to Northeastern University) were used to generate data for this manuscript. Additional support was provided by a Ford Foundation predoctoral fellowship award to ABM. All sequence data from this study is available in the Sequence Read Archive under accession number PRJNA505917. The views expressed here are those of the authors and do not necessarily reflect the views of NOAA or any of is subagencies.

ORCID

Ashley N. Bulseco https://orcid.org/0000-0001-5322-3070
Anne E. Giblin https://orcid.org/0000-0003-3851-2178
Jane Tucker https://orcid.org/0000-0002-9119-8539
Anna E. Murphy https://orcid.org/0000-0002-4904-769X
Jonathan Sanderman https://orcid.org/0000-0002-3215-1706
Kenly Hiller-Bittrolff https://orcid.org/0000-0002-6230-9404
Jennifer L. Bowen https://orcid.org/0000-0003-0339-1564

REFERENCES

Achtnich, C., Bak, F., & Conrad, R. (1995). Competition for electron donors among nitrate reducers, ferric iron reducers, sulfate reducers, and methanogens in anoxic paddy soil. *Biology and Fertility of Soils*, *19*, 65–72. https://doi.org/10.1007/BF00336349

Aller, R. C., & Aller, J. Y. (1998). The effect of biogenic irrigation intensity and solute exchange on diagenetic reaction rates in marine sediments. *Journal of Marine Research*, *56*, 905–936. https://doi.org/10.1357/002224098321667413

Allison, S. D., Lu, Y., Weihe, C., Goulden, M. L., Martiny, A. C., Treseder, K. K., & Martiny, J. B. H. (2013). Microbial abundance and composition

influence litter decomposition response to environmental change. *Ecology*, *94*, 714–725. https://doi.org/10.1890/12-1243.1

Allison, S. D., & Martiny, J. B. H. (2008). Resistance, resilience, and redundancy in microbial communities. *Proceedings of the National Academy of Sciences of the United States of America*, *105*, 11512–11519. https://doi.org/10.1073/pnas.0801925105

Allison, S. D., Weintraub, M. N., Gartner, T. B., & Waldrop, M. P. (2010). Evolutionary-economic principles as regulators of soil enzyme production and ecosystem function. In G. C. Shukla, & A. Varma (Eds.) *Soil enzymology* (pp. 245–258). Heidelbert, Germany: Springer.

Angell, J. H., Peng, X., Ji, Q., Craick, I., Jayakumar, A., Kearns, P. J., … Bowen, J. L. (2018). Community composition of nitrous oxide-related genes in salt marsh sediments exposed to nitrogen enrichment. *Frontiers in Microbiology*, *9*, 170. https://doi.org/10.3389/fmicb.2018.00170

Arndt, S., Jørgensen, B. B., LaRowe, D. E., Middelburg, J. J., Pancost, R. D., & Regnier, P. (2013). Quantifying the degradation of organic matter in marine sediments: A review and synthesis. *Earth-Science Reviews*, *123*, 53–86. https://doi.org/10.1016/j.earscirev.2013.02.008

Artz, R. R. E., Chapman, S. J., Robertson, A. H., Potts, J. M., Laggoun-Défarge, F., Gogo, S., … Francez, A. (2008). FTIR spectroscopy can predict organic matter quality in regenerating cutover peatlands. *Soil Biology and Biochemistry*, *40*, 515–527.

Bahr, M., Crump, B. C., Klepac-Ceraj, V., Teske, A., Sogin, M. L., & Hobbie, J. E. (2005). Molecular characterization of sulfate-reducing bacteria in a New England salt marsh. *Environmental Microbiology*, *7*, 1175–1185. https://doi.org/10.1111/j.1462-2920.2005.00796.x

Beauchamp, E., Trevors, J., & Paul, J. W. (1989). Carbon sources for bacterial denitrification. *Advances in Soil Science*, *10*, 113–142.

Benner, R., Newell, S. Y., Maccubbin, A. E., & Hodson, R. E. (1984). Relative contributions of bacteria and fungi to rates of degradation of lignocellulosic detritus in salt-marsh sediments. *Applied and Environmental Microbiology*, *48*, 36–40.

Biebl, H., & Pfening, N. (1981). Isolation of members of the family Rhodospirillaceae. In M. Starr, H. Stolp, H. Truper, A. Balows, & H. Schlegel (Eds.), *The prokaryotes* (pp. 267–268). Berlin, Heidelberg: Springer.

Bricker, S. B., Longstaff, B., Dennison, W., Jones, A., Boicourt, K., Wicks, C., & Woerner, J. (2008). Effects of nutrient enrichment in the nation's estuaries: A decade of change. *Harmful Algae*, *8*, 21–32. https://doi.org/10.1016/j.hal.2008.08.028

Brodowski, S., John, B., Flessa, H., & Amelung, W. (2006). Aggregate-occluded black carbon in soil. *European Journal of Soil Science*, *57*, 539–546. https://doi.org/10.1111/j.1365-2389.2006.00807.x

Brunet, R. C., & Garcia-Gil, L. J. (1996). Sulfide-induced dissimilatory nitrate reduction to ammonia in anaerobic freshwater sediments. *FEMS Micrbiology Ecology*, *21*, 131–138. https://doi.org/10.1111/j.1574-6941.1996.tb00340.x

Callahan, B. J., McMurdie, P. J., Rosen, M. J., Han, A. W., Johnson, A. J. A., & Holmes, S. P. (2016). DADA2: High-resolution sample inference from Illumina amplicon data. *Nature Methods*, *13*, 581–583. https://doi.org/10.1038/nmeth.3869

Campbell, B. J., Polson, S. W., Hanson, T. E., Mack, M. C., & Schuur, E. A. G. (2010). The effect of nutrient deposition on bacterial communities in Arctic tundra soil. *Environmental Microbiology*, *12*, 1842–1854. https://doi.org/10.1111/j.1462-2920.2010.02189.x

Canfield, D. (1989). Sulfate reduction and oxic respiration in marine sediments: Implications for organic carbon preservation in euxinic environments. *Deep Sea Research Part A: Oceanogorahic Research Papers*, *36*, 121–138. https://doi.org/10.1016/0198-0149(89)90022-8

Canfield, D. E., & Farquhar, J. (2009). Animal evolution, bioturbation, and the sulfate concentration of the oceans. *Proceedings of the National Academy of Sciences of the United States of America*, *106*, 8123–8127. https://doi.org/10.1073/pnas.0902037106

Canfield, D. E., Thamdrup, B., & Kristensen, E. (2005). *Aquatic geomicrobiology*. A. J. Southward, P. A. Tyler, C. M. Young, & L. A. Fuiman (Eds.). Boston, MA: Elsevier Academic Press.

Caporaso, J. G., Lauber, C. L., Walters, W. A., Berg-Lyons, D., Huntley, J., Fierer, N., … Knight, R. (2012). Ultra-high-throughput microbial community analysis on the Illumina HiSeq and MiSeq platforms. *The ISME Journal*, *6*, 1621–1624. https://doi.org/10.1038/ismej.2012.8

Caporaso, J. G., Lauber, C. L., Walters, W. A., Berg-Lyons, D., Lozupone, C. A., Turnbaugh, P. J., … Knight, R. (2011). Global patterns of 16S rRNA diversity at a depth of millions of sequences per sample. *Proceedings of the National Academy of Sciences of the United States of America*, *108*, 4516–4522. https://doi.org/10.1073/pnas.1000080107

Chmura, G. L., Anisfeld, S. C., Cahoon, D. R., & Lynch, J. C. (2003). Global carbon sequestration in tidal, saline wetland soils. *Global Biogeochemical Cycles*, *17*, 1–12. https://doi.org/10.1029/2002GB001917

Coolon, J. D., Jones, K. L., Todd, T. C., Blair, J. M., & Herman, M. A. (2013). Long-term nitrogen amendment alters the diversity and assemblage of soil bacterial communities in tallgrass prarie. *PLoS ONE*, *8*, e67884.

Cox, R. D. (1980). Determination of nitrate and nitrite at the parts per billion level by chemiluminescence. *Analytical Chemistry*, *52*, 332–335. https://doi.org/10.1021/ac50052a028

Dalsgaard, T., Thamdrup, B., & Canfield, D. E. (2005). Anaerobic ammonium oxidation (anammox) in the marine environment. *Research in Microbiology*, *156*, 457–464. https://doi.org/10.1016/j.resmic.2005.01.011

Dargusch, P., & Thomas, S. (2012). A critical role for carbon offsets. *Nature Climate Change*, *2*, 470–470. https://doi.org/10.1038/nclimate1578

Deegan, L. A., Bowen, J. L., Drake, D., Fleeger, J. W., Friedrichs, C. T., Galván, K. A., … Hopkinson, C. (2007). Susceptibility of salt marshes to nutrient enrichment and predation removal. *Ecological Applications*, *17*, 42–63.

Deegan, L. A., Johnson, D. S., Warren, R. S., Peterson, B. J., Fleeger, J. W., Fagherazzi, S., & Wollheim, W. M. (2012). Coastal eutrophication as a driver of salt marsh loss. *Nature*, *490*, 388–392. https://doi.org/10.1038/nature11533

Dell'Anno, A., & Danavaro, R. (2005). Extracellular DNA plays a key role in deep-sea ecosystem functioning. *Science*, *309*, 2179–2179. https://doi.org/10.1126/science.1117475

Dickson, A. G., & Goyet, C. (1994). Handbook of methods for the analysis of various parameters of the carbon dioxide system in sea water; version 2. DOE ORNL/CDIAC 74.

Duarte, C. M., Middelburg, J. J., & Caraco, N. (2005). Major role of marine vegetation on the oceanic carbon cycle. *Biogeosciences*, *2*, 1–8. https://doi.org/10.5194/bg-2-1-2005

Eppinger, M., Baar, C., Raddatz, G., Huson, D. H., & Schuster, S. C. (2004). Comparative analysis of four Campylobacterales. *Nature Reviews Microbiology*, *2*, 872–885. https://doi.org/10.1038/nrmicro1024

Eyre, B. D., Rysgaard, S., Dalsgaard, T., & Christensen, P. B. (2002). Comparison of isotope pairing and N2: Ar methods for measuring sediment denitrification – Assumptions, modifications, and implications. *Estuaries*, *25*, 1077–1087.

Falkowski, P. G., Fenchel, T., & Delong, E. F. (2008). The microbial engines that drive Earth's biogeochemical cycles. *Science*, *320*, 1034–1039. https://doi.org/10.1126/science.1153213

Fernández-Gómez, B., Richter, M., Schüler, M., Pinhassi, J., Acinas, S. G., González, J. M., & Pedrós-Alió, C. (2013). Ecology of marine bacteroidetes: A comparative genomics approach. *The ISME Journal*, *7*, 1026–1037. https://doi.org/10.1038/ismej.2012.169

Forbrich, I., Giblin, A. E., & Hopkinson, C. S. (2018). Constraining marsh carbon budgets using long-term C burial and contemporary atmospheric CO_2 fluxes. *Journal of Geophysical Research: Biogeosciences*, *123*, 867–878.

Freitas, S., Hatosy, S., Fuhrman, J. A., Huse, S. M., Mark Welch, D. B., Sogin, M. L., & Martiny, A. C. (2012). Global distribution and diversity of marine Verrucomicrobia. *The ISME Journal*, *6*, 1499–1505. https://doi.org/10.1038/ismej.2012.3

Froelich, P. N., Klinkhammer, G. P., Bender, M. L., Luedtke, N. A., Heath, G. R., Cullen, D., … Maynard, V. (1979). Early oxidation of organic matter in pelagic sediments of the eastern equatorial Atlantic: Suboxic diagenesis. *Geochimica Et Cosmochimica Acta*, *43*, 1075–1090. https://doi.org/10.1016/0016-7037(79)90095-4

Galloway, J. N., Leach, A. M., Erisman, J. W., & Bleeker, A. (2017). Nitrogen the historical progression from ignorance to knowledge with a view to future solutions. *Soil Research*, *55*, 417–424. https://doi.org/10.1071/SR16334

Galloway, J. N., Townsend, A. R., Erisman, J. W., Bekunda, M., Cai, Z., Freney, J. R., … Sutton, M. A. (2008). Transformation of the nitrogen cycle: Recent trends, questions, and potential solutions. *Science*, *320*, 889–892.

Garrity, G., Bell, J., & Lilburn, T. (2005). Thiotrichales ord nov. In D. Brenner, (Ed.), *Bergey's manual of systematic bacteriology* (2nd ed., pp. 131–210). Boston, MA: Springer.

Giblin, A., Tobias, C., Song, B., Weston, N., Banta, G., & Rivera-Monroy, V. (2013). The importance of dissimilatory nitrate reduction to ammonium (DNRA) in the nitrogen cycle of coastal ecosystems. *Oceanography*, *26*, 124–131. https://doi.org/10.5670/oceanog.2013.54

Gilboa-Garber, N. (1971). Direct spectrophotometric determination of inorganic sulfide in biological materials and in other complex mixtures. *Analytical Biochemistry*, *43*, 129–133. https://doi.org/10.1016/0003-2697(71)90116-3

Graves, C. J., Makrides, E. J., Schmidt, V. T., Giblin, A. E., Carbon, Z. G., & Rand, D. M. (2016). Functional response of salt marsh microbial communities to long-term nutrient enrichment. *Applied and Environmental Microbiology*, *82*, 2862–2871.

Guibert, L. M., Loviso, C. L., Borglin, S., Jansson, J. K., Dionisi, H. M., & Lozada, M. (2016). Diverse bacterial groups contribute to the alkane degradation potential of chronically polluted subantarctic coastal sediments. *Microbial Ecology*, *71*, 100–112. https://doi.org/10.1007/s00248-015-0698-0

Hamersley, M. R., & Howes, B. L. (2005). Coupled nitrification-denitrification measured in situ in a *Spartina alterniflora* marsh with a $^{15}NH_4^+$ tracer. *Marine Ecology Progress Series*, *299*, 123–135. https://doi.org/10.3354/meps299123

Herbert, R. A. (1999). Nitrogen cycling in coastal marine ecosystems. *FEMS Microbiology Reviews*, *23*, 563–590. https://doi.org/10.1111/j.1574-6976.1999.tb00414.x

Hopkinson, C. S., & Giblin, A. E. (2008). Nitrogen dynamics of coastal salt marshes. In D. Capone, D. Bronk, M. Mulholland, & E. Carpenter (Eds.), *Nitrogen in the marine environment* (2nd ed., pp. 991–1036). Burlington, MA: Academic Press.

Howarth, R. W. (1984). The ecological significance of sulfur in the energy dynamics of salt marsh and coastal marine sediments. *Biogeochemistry*, *1*, 5–27. https://doi.org/10.1007/BF02181118

Howarth, R. W., & Teal, J. M. (1979). Sulfate reduction in a New England salt marsh. *Limnology and Oceanography*, *24*, 999–1013.

Howes, B. L., Howarth, R. W., Teal, J. M., & Valiela, I. (1981). Oxidation-reduction potentials in a salt marsh: Spatial patterns and interactions with primary production. *Limnology and Oceanography*, *26*, 350–360.

Iino, T., Mori, K., Uchino, Y., Nakagawa, T., Harayama, S., & Suzuki, K. I. (2010). *Ignavibacterium album* gen. nov., sp. nov., a moderately thermophilic anaerobic bacterium isolated from microbial mats at a terrestrial hot spring and proposal of Ignavibacteria classis nov., for a novel lineage at the periphery of green sulfur bacteria. *International Journal of Systematic and Evolutionary Microbiology*, *60*, 1376–1382.

Imhoff, J. (2005). Bergey's manual of systematic bacteriology. In D. Brenner, N. Krieg, J. Staley, & G. Garrity (Eds.), *Bergey's manual of systematic bacteriology* (2nd ed., pp. 1–59). Boston, MA: Springer.

Jørgensen, B. B. (1977). The sulfur cycle of a coastal marine sediment (Limfjorden, Denmark). *Limnology and Oceanography*, *22*, 814–832.

Kana, T. M., Darkangelo, C., Duane Hunt, M., Oldham, J. B., Bennett, G. E., & Cornwell, J. C. (1994). Membrane inlet mass spectrometer for rapid high-precision determination of N_2, O_2, and Ar in environmental water samples. *Analytical Chemistry*, *66*, 4166–4170. https://doi.org/10.1021/ac00095a009

Kaplan, W., Valiela, I., & Teal, J. M. (1979). Denitrification in a salt marsh ecosystem. *Limnology and Oceanography*, *24*, 726–734.

Katoh, K., & Standley, D. M. (2013). MAFFT multiple sequence alignment software version 7: Improvements in performance and usability. *Molecular Biology and Evolution*, *30*, 772–780. https://doi.org/10.1093/molbev/mst010

Kearns, P. J., Angell, J. H., Howard, E., Deegan, L. A., Stanley, R. H., & Bowen, J. L. (2016). Nutrient enrichment induces high rates of dormancy and decreases diversity of active bacterial taxa. *Nature Communications*, *7*, 1–9.

Keiluweit, M., Wanzek, T., Kleber, M., Nico, P., & Fendorf, S. (2017). Anaerobic microsites have an unaccounted role in soil carbon stabilization. *Nature Communications*, *8*, 1–10. https://doi.org/10.1038/s41467-017-01406-6

Koop-Jakobsen, K., & Giblin, A. E. (2009). Anammox in tidal marsh sediments: The role of salinity, nitrogen loading, and marsh vegetation. *Estuaries and Coasts*, *32*, 238–245. https://doi.org/10.1007/s12237-008-9131-y

Koop-Jakobsen, K., & Giblin, A. E. (2010). The effect of increased nitrate loading on nitrate reduction via denitrification and DNRA in salt marsh sediments. *Limnology and Oceanography*, *55*, 789–802. https://doi.org/10.4319/lo.2010.55.2.0789

Kostka, J. E., Gribsholt, B., Petrie, E., Dalton, D., Skelton, H., & Kristensen, E. (2002). The rates and pathways of carbon oxidation in bioturbated saltmarsh sediments. *Limnology and Oceanography*, *47*, 230–240. https://doi.org/10.4319/lo.2002.47.1.0230

Kuhn, M. (2016). A short introduction to the caret package. R Foundation for Statistical Computing, 1–10. Retrieved from cran.r-project.org/web/packages/caret/vignettes/caret.pdf

Langley, J. A., Mozdzer, T. J., Shepard, K. A., Hagerty, S. B., & Megonigal, J. P. (2013). Tidal marsh plant responses to elevated CO_2, nitrogen fertilization, and sea level rise. *Global Change Biology*, *19*, 1495–1503.

Leff, J. W., Jones, S. E., Prober, S. M., Barberán, A., Borer, E. T., Firn, J. L., … Fierer, N. (2015). Consistent responses of soil microbial communities to elevated nutrient inputs in grasslands across the globe. *Proceedings of the National Academy of Sciences of the United States of America*, *112*, 10967–10972. https://doi.org/10.1073/pnas.1508382112

Liaw, A., & Wiener, M. (2002). Classification and regression by randomForest. *R News*, *2*, 18–22.

Logan, J. M. (2018). Salt marsh aboveground production in New England estuaries in relation to nitrogen loading and environmental factors. *Wetlands*, *38*, 1327–1340. https://doi.org/10.1007/s13157-018-1056-z

Lozupone, C., Lladser, M. E., Knights, D., Stombaugh, J., & Knight, R. (2011). UniFrac: An effective distance metric for microbial community comparison. *The ISME Journal*, *5*, 169–172. https://doi.org/10.1038/ismej.2010.133

Lunstrum, A., & Aoki, L. (2016). Oxygen interference with membrane inlet mass spectrometry may overestimate denitrification rates calculated with the isotope pairing technique. *Limnology and Oceanography: Methods*, *14*, 425–431.

Luther, G. III, Church, T. M., Scudlark, J. R., & Cosman, M. (1986). Inorganic and organic sulfur cycling in salt-marsh pore waters. *Science*, *232*, 746–749. https://doi.org/10.1126/science.232.4751.746

Macreadie, P. I., Nielsen, D. A., Kelleway, J. J., Atwood, T. B., Seymour, J. R., Petrou, K., … Ralph, P. J. (2017). Can we manage coastal ecosystems to sequester more blue carbon? *Frontiers in Ecology and the Environment*, *15*, 206–213. https://doi.org/10.1002/fee.1484

Mahmoudi, N., Robeson, M. S., Castro, H. F., Fortney, J. L., Techtmann, S. M., Joyner, D. C., … Hazen, T. C. (2015). Microbial community composition and diversity in Caspian Sea sediments. *FEMS Microbiology Ecology*, *91*, 1–11. https://doi.org/10.1093/femsec/fiu013

Margenot, A. J., Calderón, F. J., Bowles, T. M., Parikh, S. J., & Jackson, L. E. (2015). Soil organic matter functional group composition in relation to organic carbon, nitrogen, and phosphorus fractions in organically managed tomato fields. *Soil Science Society of America Journal*, *79*, 772–782. https://doi.org/10.2136/sssaj2015.02.0070

McCarren, J., Becker, J. W., Repeta, D. J., Shi, Y., Young, C. R., Malmstrom, R. R., … DeLong, E. F. (2010). Microbial community transcriptomes reveal microbes and metabolic pathways associated with dissolved organic matter turnover in the sea. *Proceedings of the National Academy of Sciences of the United States of America*, *107*, 16420–16427. https://doi.org/10.1073/pnas.1010732107

McDonald, D., Price, M. N., Goodrich, J., Nawrocki, E. P., DeSantis, T. Z., Probst, A., … Hugenholtz, P. (2012). An improved Greengenes taxonomy with explicit ranks for ecological and evolutionary analyses of bacteria and archaea. *ISME Journal*, *6*, 610–618. https://doi.org/10.1038/ismej.2011.139

Mcleod, E., Chmura, G. L., Bouillon, S., Salm, R., Björk, M., Duarte, C. M., … Silliman, B. R. (2011). A blueprint for blue carbon: Toward an improved understanding of the role of vegetated coastal habitats in sequestering CO_2. *Frontiers in Ecology and the Environment*, *9*, 552–560.

Meyer, A. F., Lipson, D. A., Martin, A. P., Schadt, C. W., & Schmidt, S. K. (2004). Molecular and metabolic characterization of cold-tolerant alpine soil pseudomonas sensu stricto. *Applied and Environmental Microbiology*, *70*, 483–489. https://doi.org/10.1128/AEM.70.1.483-489.2004

Michener, C. D., & Sokal, R. R. (1957). A quantitative approach to a problem in classification. *Evolution*, *11*, 130–162. https://doi.org/10.1111/j.1558-5646.1957.tb02884.x

Miroshnichenko, M. L., Kolganova, T. V., Spring, S., Chernyh, N., & Bonch-Osmolovskaya, E. A. (2010). *Caldithrix palaeochoryensis* sp. nov., a thermophilic, anaerobic, chemo-organotrophic bacterium from a geothermally heated sediment, and emended description of the genus Caldithrix. *International Journal of Systematic and Evolutionary Microbiology*, *60*, 2120–2123.

Morris, J. T., Sundareshwar, P. V., Nietch, C. T., Kjerfve, B., & Cahoon, D. R. (2002). Responses of coastal wetlands to rising sea level. *Ecology*, *83*, 2869–2877. https://doi.org/10.1890/0012-9658(2002)083[2869:ROCWTR]2.0.CO;2

Negrin, V. L., Spetter, C. V., Asteasuain, R. O., Perillo, G. M., & Marcovecchio, J. E. (2011). Influence of flooding and vegetation on carbon, nitrogen, and phosphorus dynamics in the pore water of a *Spartina alterniflora* salt marsh. *Journal of Environmental Sciences*, *23*, 212–221. https://doi.org/10.1016/S1001-0742(10)60395-6

Nelleman, C., Corcoran, E., Duarte, C., Valdes, L., DeYoung, C., Foncesa, L., & Grimsditch, G. (2009). Blue carbon: A rapid response assessment. Arendal, Norway: United Nations Environment Programme.

Neubauer, S. C., & Megonigal, J. P. (2015). Moving beyond global warming potentials to quantify the climatic role of ecosystems. *Ecosystems*, *18*, 1000–1013.

Nielsen, L. P. (1992). Denitrification in sediment determined from nitrogen isotope pairing. *FEMS Microbiology Ecology*, *9*, 357–361. https://doi.org/10.1111/j.1574-6941.1992.tb01771.x

Pallud, C., Meile, C., Laverman, A. M., Abell, J., & Van Cappellen, P. (2007). The use of flow-through sediment reactors in biogeochemical kinetics: Methodology and examples of applications. *Marine Chemistry*, *106*, 256–271.

Pallud, C., & Van Cappellen, P. (2006). Kinetics of microbial sulfate reduction in estuarine sediments. *Geochimica Et Cosmochimica Acta*, *70*, 1148–1162. https://doi.org/10.1016/j.gca.2005.11.002

Parikh, S. J., Goybe, K. W., Margenot, A. J., Mukome, F. N. D., & Calderón, F. J. (2014). Soil chemical insights provided through vibrational spectroscopy. *Advances in Agronomy*, *126*, 1–148.

Pastore, M. A., Megonigal, J. P., & Langley, J. A. (2017). Elevated CO_2 and nitrogen addition accelerate net carbon gain in a brackish marsh. *Biogeochemistry*, *133*, 73–87. https://doi.org/10.1007/s10533-017-0312-2

Peng, X., Ji, Q., Angell, J. H., Kearns, P. J., Yang, H. J., Bowen, J. L., & Ward, B. B. (2016). Long-term fertilization alters the relative importance of nitrate reduction pathways in salt marsh sediments. *Journal of Geophysical Research: Biogeosciences*, *121*, 2082–2095. https://doi.org/10.1002/2016JG003484

R Core Team. (2019). *R: A language and environment for statistical computing*. Vienna, Austria: R Foundation for Statistical Computing. Retrieved from http://www.R-project.org

Reddy, K., & Patrick, W. Jr. (1975). Effect of alternate aerobic and anaerobic conditions on redox potential, organic matter decomposition, and nitrogen loss in a flooded soil. *Soil Biology and Biochemistry*, *7*, 87–94. https://doi.org/10.1016/0038-0717(75)90004-8

Reese, B. K., Witmer, A. D., Moller, S., Morse, J. W., & Mills, H. J. (2013). Molecular assays advance understanding of sulfate reduction despite cryptic cycles. *Biogeochemistry*, *118*, 307–319. https://doi.org/10.1007/s10533-013-9933-2

Ryther, J. H., & Dunstan, W. M. (1971). Nitrogen, phosphorus, and eutrophication in the coastal marine environment. *Science*, *171*, 1008–1013. https://doi.org/10.1126/science.171.3975.1008

Schmid, M. C., Risgaard-Petersen, N., van de Vossenberg, J., Kuypers, M. M. M., Lavik, G., Petersen, J., … Jetten, M. S. M. (2007). Anaerobic ammonium-oxidizing bacteria in marine environments: Widespread occurrence but low diversity. *Environmental Microbiology*, *9*, 1476–1484. https://doi.org/10.1111/j.1462-2920.2007.01266.x

Schmidt, M. W. I., Torn, M. S., Abiven, S., Dittmar, T., Guggenberger, G., Janssens, I. A., … Trumbore, S. E. (2011). Persistence of soil organic matter as an ecosystem property. *Nature*, *478*, 49. https://doi.org/10.1038/nature10386

Shade, A., Peter, H., Allison, S. D., Baho, D. L., Berga, M., Bürgmann, H., … Handelsman, J. (2012). Fundamentals of microbial community resistance and resilience. *Frontiers in Microbiology*, *3*, 1–19.

Solórzano, L. (1969). Determination of ammonia in natural waters by the phenolhypochlorite method. *Limnology and Oceanography*, *14*, 799–801.

Thamdrup, B., & Dalsgaard, T. (2002). Production of N2 through anaerobic ammonium oxidation coupled to nitrate reduction in marine sediments. *Applied and Environmental Microbiology*, *68*, 1312–1318.

Thomas, F., Giblin, A. E., Cardon, Z. G., & Sievert, S. M. (2014). Rhizosphere heterogeneity shapes abundance and activity of sulfur-oxidizing bacteria in vegetated salt marsh sediments. *Frontiers in Microbiology*, *5*, 309. https://doi.org/10.3389/fmicb.2014.00309

Treseder, K. K., Kivlin, S. N., & Hawkes, C. V. (2011). Evolutionary trade-offs among decomposers determine responses to nitrogen enrichment. *Ecology Letters*, *14*, 933–938. https://doi.org/10.1111/j.1461-0248.2011.01650.x

Valiela, I., & Cole, M. L. (2002). Comparative evidence that salt marshes and mangroves may protect seagrass meadows from land-derived nitrogen loads. *Ecosystems*, *5*, 92–102. https://doi.org/10.1007/s10021-001-0058-4

Valiela, I., & Teal, J. M. (1974). Nutrient limitation in salt marsh vegetation. In R. J. Reimold, & W. H. Queen (Eds.), *Ecology of halophytes* (pp. 547–563). New York, NY: Academic Press.

Vivanco, L., Irvine, I. C., & Martiny, J. B. H. (2015). Nonlinear responses in salt marsh functioning to increased nitrogen addition. *Ecology*, *96*, 936–947. https://doi.org/10.1890/13-1983.1

Warren, R. S., Fell, P. E., Rozsa, R., Brawley, A. H., Orsted, A. C., Olson, E. T., … Niering, W. A. (2002). Salt marsh restoration in Connecticut: 20 years of science and management. *Restoration Ecology*, *10*, 497–513. https://doi.org/10.1046/j.1526-100X.2002.01031.x

Westrich, J. T., & Berner, R. A. (1984). The role of sedimentary organic matter in bacterial sulfate reduction: The G model tested. *Limnology and Oceanography*, *29*, 236–249.

Wiese, J., Thiel, V., Gärtner, A., Schmaljohann, R., & Imhoff, J. F. (2009). *Kiloniella laminariae* gen. nov., sp. nov., an alphaproteobacterium from the marine macroalga *Laminaria saccharina*. *International Journal of Systematic and Evolutionary Microbiology*, *59*, 350–356.

Wigand, C., Brennan, P., Stolt, M., Holt, M., & Ryba, S. (2009). Soil respiration rates in coastal marshes subject to increasing watershed nitrogen loads in southern New Engand, USA. *Wetlands*, *29*, 952–963.

Wilson, C. A., Hughes, Z. J., FitzGerald, D. M., Hopkinson, C. S., Valentine, V., & Kolker, A. S. (2014). Saltmarsh pool and tidal creek morphodynamics: Dynamic equilibrium of northern latitude saltmarshes? *Geomorphology*, *213*, 99–115. https://doi.org/10.1016/j.geomorph.2014.01.002

Yin, G., Hou, L., Liu, M., Liu, Z., & Gardner, W. S. (2014). A novel membrane inlet mass spectrometer method to measure $^{15}NH_4^+$ for isotope-enrichment experiments in aquatic ecosystems. *Environmental Science & Technology*, *48*, 9555–9562.

Zehnder, A., & Stumm, W. (1988). Geochemistry and biogeochemistry of anaerobic habitats. In A. Zehnder (Ed.), *Biology of anaerobic microorganisms* (pp. 1–38). New York, NY: Wiley.

SUPPORTING INFORMATION

Additional supporting information may be found online in the Supporting Information section at the end of the article.

How to cite this article: Bulseco AN, Giblin AE, Tucker J, et al. Nitrate addition stimulates microbial decomposition of organic matter in salt marsh sediments. *Glob Change Biol*. 2019;00:1–18. https://doi.org/10.1111/gcb.14726